F 24P

NASA TECHNICAL NOTE

NASA TN D-7699

NASA TN D-7699

EVALUATION OF ALLOYS AND COATINGS FOR USE IN AUTOMOBILE THERMAL REACTORS

by Charles P. Blankenship and Robert E. Oldrieve

Lewis Research Center
Cleveland, Ohio 44135

NATIONAL AERONAUTICS AND SPACE ADMINISTRATION • WASHINGTON, D. C. • JULY 1974

1. Report No.	2. Government Accession No.	3. Recipient's Catalog No.
NASA TN D-7699		

4. Title and Subtitle	5. Report Date
EVALUATION OF ALLOYS AND COATINGS FOR USE IN AUTOMOBILE THERMAL REACTORS	JULY 1974
	6. Performing Organization Code

7. Author(s)	8. Performing Organization Report No.
Charles P. Blankenship and Robert E. Oldrieve	E-7856
	10. Work Unit No. 501-21

9. Performing Organization Name and Address	11. Contract or Grant No.
Lewis Research Center National Aeronautics and Space Administration Cleveland, Ohio 44135	

12. Sponsoring Agency Name and Address	13. Type of Report and Period Covered
National Aeronautics and Space Administration Washington, D.C. 20546	Technical Note
	14. Sponsoring Agency Code

15. Supplementary Notes

16. Abstract

Several candidate alloys and coatings were evaluated for use in automobile thermal reactors. Full-size reactors of the candidate materials were evaluated in cyclic engine dynamometer tests with a peak temperature of 1040° C (1900° F). Two developmental ferritic-iron alloys, GE-1541 and NASA-18T, exhibited the best overall performance by lasting at least 60 percent of the life of the test engine. Four of the alloys evaluated warrant consideration for reactor use. They are GE-1541, Armco 18 SR, NASA-18T, and Inconel 601. None of the commercial coating substrate combinations evaluated warrant consideration for reactor use.

17. Key Words (Suggested by Author(s))	18. Distribution Statement
Ferritic-iron alloys Emission control devices Materials for emission control devices Alloy coatings	Unclassified - unlimited Category 17

19. Security Classif. (of this report)	20. Security Classif. (of this page)	21. No. of Pages	22. Price*
Unclassified	Unclassified	50	$3.25

* For sale by the National Technical Information Service, Springfield, Virginia 22151

CONTENTS

EVALUATION OF ALLOYS AND COATINGS FOR USE IN AUTOMOBILE THERMAL REACTORS

by Charles P. Blankenship and Robert E. Oldrieve

Lewis Research Center

SUMMARY

An evaluation was made of several candidate alloys and coatings for use in automobile thermal reactors. Emphasis was placed on low cost ferritic-iron alloys and commercial coatings on an AISI 651 (19-9DL) substrate. Inconel 601 was included as a relatively low cost nickel-base alloy having potential for reactor use. Full-size thermal reactors fabricated from the candidate materials were evaluated in engine-dynamometer screening and endurance tests. The test reactors were subjected to cyclic operation with exposure at a peak metal temperature of 1040° C (1900° F) for at least 50 percent of the total test time. The performance of the candidate materials was based on the relative resistance of the reactor test cores to oxidation, erosion, and distortion.

Two developmental ferritic-iron alloys, GE-1541 (Fe-15Cr-4Al-1Y) and NASA-18T (Fe-18Cr-2Al-1Si-1.25Ta), exhibited the best overall performance. At the end of this program test reactors of these alloys had completed successfully about 700 hours of endurance testing without failure. This represents about 60 to 70 percent of the engine life under the endurance test conditions. Reactor core weight loss was less than 1 percent. Another ferritic-iron alloy, Armco 18 SR (Fe-18Cr-2Al-1Si), performed reasonably well for about 600 hours of the endurance test. Because localized oxidation was extensive, penetration of the test reactor core resulted. However, total reactor core weight loss was less than 2 percent.

Inconel 601, included in the program for comparative purposes, was endurance tested for 1000 hours. However, at comparable test times (e.g., 700 hr), the Inconel 601 test reactor core exhibited greater weight loss than the ferritic-iron alloys, and it distorted more than the GE-1541 reactor core.

None of the commercial coatings evaluated survived more than 325 hours of endurance testing. These coatings were Cr-Al, Ni-Cr, and glass-ceramic type coatings on an AISI 651 substrate. Reactor core failure was due primarily to a failure of the coatings. An uncoated reactor core of the more oxidation resistant alloy AISI 310 failed in less than 500 hours of endurance testing. This failure was attributed to general oxidation and corrosion with the core weight loss exceeding 20 percent.

Of the alloys evaluated GE-1541, Armco 18 SR, NASA-18T, and Inconel 601 warrant consideration for reactor use. On the basis of lower cost and fabricability, preference should be given to the Armco 18 SR and the NASA-18T alloys.

INTRODUCTION

Thermal reactors have been shown to be an effective means of reducing exhaust gas pollutants from automobile engines (refs. 1 to 5). A thermal reactor is essentially a close-coupled afterburner (installed in place of the cast-iron exhaust manifold) into which air is injected to oxidize unburned hydrocarbons and carbon monoxide. During the oxidation process the core of the reactor reaches temperatures from about 870° to 1040° C (1600° to 1900° F) under normal driving conditions. This high-temperature oxidizing environment in combination with high-velocity corrosive constituents in the exhaust gas presents a severe environment for reactor materials. Of particular concern has been the inability of low-cost, abundantly available materials to survive the reactor environment for long time periods (ref. 6).

The program reported herein is a part of an overall evaluation of potential materials for thermal reactor use (ref. 7). In this evaluation of alloys and coatings emphasis was placed on determining the performance of low-cost ferritic-iron alloys of the iron-chromium-aluminum (Fe-Cr-Al) type and potentially low-cost coatings on an austenitic-iron alloy substrate. More expensive, nickel-base superalloys having a potential for reactor use were included for comparative purposes. Specific alloys and coatings included in this evaluation were selected in part on the basis of coupon-type thermal reactor screening tests of many candidate materials (refs. 3 and 8).

Full-size thermal reactors of the candidate materials were used in this evaluation program. The test reactors were subjected to either or both screening and endurance tests on automotive engine-dynamometer test stands. The reactor tests were cyclic with exposure to a peak metal temperature of 1040° C (1900° F) in nearly all the tests for at least 50 percent of the test time. The performance of the alloys and coatings was based on the relative resistance of the reactor test cores to oxidation, erosion, and distortion. The alloys and coatings included in the evaluation, test reactor design, test conditions, and the results are described in this report.

Over 11 000 reactor test hours were accumulated in conducting this evaluation. Fabrication and engine testing of the reactors were accomplished under a NASA contract with the Teledyne-Continental Motors Division of Teledyne Industries. This program was conducted in cooperation with the Office of Air Programs of the Environmental Protection Agency.

MATERIALS AND PROCEDURE

Alloys and Coatings Evaluated

The four classes of materials selected for this evaluation are ferritic-iron alloys, austenitic-iron alloys, metallic and ceramic coatings, and nickel-base superalloys. Alloy compositions and sheet gages are given in table I. Coating compositions and application details are given in table II. The key designations used in these tables are used to identify the reactor materials throughout this report. The materials were selected on the basis of their performance in prior screening tests (refs. 4 and 8) or for other reasons as described in the following sections.

Ferritic-iron alloys. - Two ferritic-iron alloys, GE-1541 and Armco 18 SR, were selected based on their availability in the sheet sizes required, adequate fabricability, and excellent oxidation resistance (refs. 9 and 10). GE-1541 is a developmental alloy, while Armco 18 SR is a commercially available alloy.

Modifications to the two ferritic alloys were made to our specifications in an attempt to improve their high-temperature strength primarily by adding 1 to 2 percent tantalum as a solid-solution strengthener. In addition, yttrium was deleted from the modified GE-1541 alloys for cost savings and also in an attempt to improve formability. Modified alloys of the GE-1541 composition, designated NASA-15T and NASA-15T2, contained about 1 or 2 percent tantalum and no yttrium (table I). In addition, the aluminum content of the NASA-15T2 alloy was increased in an attempt to provide for added oxidation resistance in the absence of yttrium. The modified alloy of Armco 18 SR, designated NASA-18T, contained 1.25 percent tantalum (table I).

Austenitic-iron alloys. - Three austenitic-iron alloys were included in the evaluation, AISI 310, AISI 651, and Incoloy 800. AISI 310 was selected because it is one of the more oxidation resistant austenitic alloys and because it had been evaluated previously by other investigators in other types of thermal reactor tests (refs. 3 and 4). AISI 651, one of the stronger and lower cost austenitic alloys, was selected for the substrate in most of the reactor coating evaluations. This alloy was judged to have sufficient strength to preclude mechanical failure of the test reactors and thereby provide a clear evaluation of the candidate coatings. Also, if successful, such a coating system might provide a candidate reactor material of intermediate cost (between ferritics and nickel-base alloys). Incoloy 800 was evaluated only as a coated reactor, since coated Incoloy 800 exhibited good performance in another type of thermal reactor test (ref. 3).

Nickel-base alloys. - The two nickel-base alloys Hastelloy X and Inconel 601 were included in the evaluation for comparative purposes. Most of the testing was performed with the lower cost Inconel 601. The latter alloy performed well in screening tests (refs. 4 and 8) and in another type of full-size reactor test (ref. 1).

Coatings. - All of the coatings selected for evaluation were developed for aircraft turbine engine components and are commercially available. Many of the coatings are proprietary. They are listed in table II by coating type, method of application, amount of coating deposited, coating vendor, and trade name. They include chromium-aluminum (Cr-Al), nickel-chromium (Ni-Cr), and ceramic-type coatings on the AISI 651 substrate. The Al coated Incoloy 800 and the Cr-Al coated AISI 310 were evaluated based on their good performance in another type of reactor materials test (ref. 3).

Reactor Design and Fabrication

Reactor design. - The test reactor design used in this program is illustrated in figures 1 and 2. This design is similar to the DuPont type II, circumferential flow reactor which has been shown to be effective in controlling exhaust emissions (refs. 2 and 3). Exhaust gases from the engine and injected air are directed to the reactor core through the port tubes. Holes in the core provide a passage for the hot gases to the annulus between the core and liner with subsequent passage for the exhaust gases through the outlet port.

To facilitate dismantling for periodic inspection the liner and the cast-iron housing were split longitudinally. This arrangement provided for easy installation and removal of the reactor test cores. Primary support of the reactor test cores was achieved by the end pins which were free to move in the housing to allow for expansion and contraction of the cores with minimal restraint. For each test reactor, the loose-fitting port tubes, the liner, and the core were fabricated from the material under evaluation. The core pins were fabricated from AISI 310. Meehanite type SF60 ductile iron was used to manufacture the split reactor housing. A fibrous type insulation was used between the liner and the cast-iron housing.

Four tubular studs on the exterior of the reactor core and opposite the exhaust inlet ports served as guides and shields for the spring-loaded thermocouples used to measure the core-metal temperatures. Some reactor core distortion was introduced by this conveniently replaceable means of sensing reactor core temperatures. Loose-fitting port tubes were used to allow for free expansion and contraction of the test reactor cores. Also, the port tubes were changed frequently for determination of material performance at the reactor inlet locations.

Reactor fabrication. - All reactor components were fabricated from sheet material of the alloy being evaluated. The austenitic-iron alloys and the nickel-base alloys were cold formed, welded, and stress-relief annealed by standard shop practices without difficulty. However, the ferritic-iron alloys GE-1541, NASA-15T, and NASA-15T2 had to be warm formed. Parts were torch heated to about 300^{o} C (600^{o} F) and then formed

into the desired shape. Formability of both Armco 18 SR and NASA-18T was sufficient for cold forming the reactor parts. For most of the ferritic-iron alloys, a special weld rod alloy designated W-1 was used to provide better oxidation and erosion resistant weldments. The W-1 composition was nominally Fe-23Cr-5Al. The weld rod for the other alloys had the same composition as the parent material except for the AISI 651 which was welded with AISI 349 welding rod.

For the coated reactors, the reactor components were coated by commercial vendors after fabrication. The components were measured and weighed before and after coating to determine the amount of coating deposited.

Engine-Dynamometer Test Procedure

Standard V-8 passenger car engines equipped with air pumps were used in this evaluation. Test reactors were installed in place of the cast-iron manifolds. All aspects of the testing program were directed toward obtaining reproducible test conditions. All the tests were conducted on identical engines with automatically controlled speeds, loads, and test cycles. The peak reactor metal temperature was controlled at nominally 1090° C (1900° F). In addition to the air supplied by the engine air pumps, supplemental air was provided to the reactors for temperature control. During operation supplemental air was automatically introduced about 10 to 20 times per hour. With the introduction of supplemental air the temperature climbed steadily until an over-temperature set point of about 1050° C (1925° F) interrupted the supplemental air flow and caused the temperature to drop to about 1025° C (1875° F). With the peak reactor temperature controlled within 30° C (50° F), temperature gradients along the length of the test reactors were as high as 100° C (200° F). The temperature gradients were approximately the same in all the tests and for all the materials evaluated. This type of peak temperature control and the resultant temperature gradients were considered acceptable for this type of materials evaluation. The engine-dynamometer test stands and the test cycles used in this evaluation are described in the following sections.

Engine-dynamometer test stands. - The 1970 V-8 engines used in this evaluation were rated at 158 kilowatts (210 hp) at 4600 rpm. Test reactors were installed as illustrated in figure 2. An eddy current dynamometer, clutch, and reverse rotation slave engine (marine version of the test engines) were used to provide simulated vehicle loading. Figure 3 shows one of the three engine-dynamometer test stands used in conducting this program.

To regulate engine operation for the cyclic testing, a punched paper-tape controller provided throttle adjustment by using pneumatic actuators and clutch engagement and throttle control for the motoring engine. Automatic recycling was accomplished by inputs provided by the time-controlled punched tape.

Screening test conditions. - Two types of tests to be used in sequence were planned to provide material screening. Engine operating conditions were adjusted to provide the test conditions and peak cycle temperature for the two screening tests which are outlined as follows:

Accelerated creep and corrosion (AC/C) test:

(1) Heat to 1040° C (1900° F).

(2) Hold at 1040° C (1900° F) for 2 hours.

(3) Idle engine 5 minutes with quench air to about 200° C (390° F).

(4) Continue air cooling with engines off for 15 minutes to about 70° C (160° F).

(5) Repeat cycle to attain at least 80 cycles in 200 hours of engine operation.

Thermal cycle (TC) test:

(1) Heat to 1040° C (1900° F) in 2 minutes or less.

(2) Hold at 1040° C (1900° F) for 10 minutes.

(3) Cut fuel flow.

(4) Cool for 3 minutes (with air injection and engine motoring) to about 370° C (700° F).

(5) Continue cooling at least 5 more minutes to about 150° C (300° F).

(6) Repeat cycle for up to 200 cycles.

The purpose of the accelerated creep and corrosion (AC/C) tests, as the name implies, was to provide sufficient time at temperature each cycle to allow significant amounts of corrosion and creep to occur. It was planned that the AC/C test would allow screening of the oxidation resistance of coated materials with minimum effects from rapid cycling. The best materials which survived AC/C testing would then be subjected to the thermal cyclic (TC) testing to determine if the candidates were prone to failure in rapid cycling. In the course of the program, however, it was determined that the AC/C test resulted in greater core weight changes, core distortion, and visually apparent damage than did equivalent test durations using the TC test. This is illustrated in figure 4 where the weight changes of two reactor core materials are compared under both test conditions. Thus, the TC test was discontinued, and all other reactor screening tests used the AC/C test cycle.

The engine operating conditions that provided the 1040° C (1900° F) reactor core temperature for the AC/C test cycle are given in table III. A schematic of the AC/C test cycle is shown in figure 5(a). All of the screening tests were conducted using commercial leaded gasoline (about 2 to 3 g of lead per 3.8×10^{-3} m^3 (gallon), 0.2 theories phosphorus, and 0.05 percent sulphur). The test reactors were given about an 8-hour soak at ambient temperature after each 16 hours of engine testing.

Endurance test conditions. - Alloys and coatings that showed good performance in the screening tests and some other selected alloys were subjected to an endurance test cycle. The endurance test cycle was designed to simulate actual driving conditions.

However, acceleration and deceleration during the test cycles were probably more rapid than would be experienced during normal vehicle operation.

A schematic of the endurance test cycle and the corresponding reactor core temperatures are presented in figure 5(b). This test cycle was intended to simulate actual driving conditions. A representation of a simulated drive to work (A) at 56 kilometers per hour (35 mph) with several stops and starts and a 10-minute drive on a freeway at 112 kilometers per hour (70 mph) is shown in figure 5(b). Representations are also shown of weekend shopping (B) and a weekend trip (C) consisting of mostly freeway driving at 112 kilometers per hour (70 mph). In addition, two 3-hour runs were used to simulate driving a vehicle pulling a trailer at 112 kilometers per hour (70 mph) on an expressway. One complete endurance test cycle was 32.5 hours long and consisted specifically of the following parts conducted in the sequence A, B, A, C, A, B, A, and C:

A:

(1) Start engine, idle 1/2 minute, accelerate to rpm equivalent of 56 kilometers per hour (35 mph), hold for 1 minute, and then decelerate to idle. Simulated vehicle weight is 1815 kilograms (4000 lb).

(2) Repeat (1) four times.

(3) Accelerate from idle to rpm equivalent to 112 kilometers per hour (70 mph), hold for 10 minutes, decelerate to idle.

(4) Repeat (1) five times and then turn engine off.

(5) Repeat (1) to (4) nine times to equal one work week.

B:

(1) Repeat (1) (from A) ten times with engine turned off between each step.

C:

(1) Start engine, accelerate to rpm equivalent to 112 kilometers per hour (70 mph), hold for 3 hours, and then decelerate to engine off. Simulated vehicle weight is 1815 kilograms (4000 lb).

(2) Repeat B.

(3) Repeat (1) with a simulated vehicle weight of 1815 kilograms (4000 lb) plus a simulated trailer weight of 900 kilograms (2000 lb).

Supplemental heating air for the reactors was applied only in the 112 kilometer per hour (70 mph) modes, and reactor wall temperatures were maintained at 1040° C (1900° F). In the 56 kilometer per hour (35 mph) mode reactor air was from the engine air pump only and was measured at 0.7 kilogram per minute (1.6 lb/min) at ambient temperature. In the 112 kilometer per hour (70 mph) modes reactor air from the air pump was about 0.5 kilogram per minute (1 lb/min), and supplemental air was added to make a total air delivery to the reactor of about 1.2 kilograms per minute (2.6 lb/min). Engine operating conditions for this endurance test cycle are tabulated in table IV. Average vehicle speed (simulated) during this test cycle was about 80 kilometers per hour (50 mph).

For approximately 18.5 hours of the 32.5-hour test cycle the reactor test cores were subjected to the peak test temperature (1040° C (1900° F)). After each 16 hours of engine testing the reactors were given an 8-hour soak at ambient temperature.

The endurance test cycle was initiated using leaded fuel identical to that fuel used in the screening tests. Early in the endurance testing phase of this program, however, a change was made to nonleaded fuel (about 0.04 g of lead per 3.8×10^{-3} m^3 (gallon), nil phosphorus, and 0.04 percent sulphur). This change was made primarily to accommodate concurrent testing of ceramic thermal reactors (ref. 11), some of which might have been subject to lead attack.

Evaluation Procedure

The relative performance of the materials evaluated was based on reactor core weight change, core distortion, visual appearance of the coatings, and metallographic evaluation. Specific measurements and measurement intervals in each type of test are described in the following sections. The following etchants were used in the metallographic evaluation:

Alloy	Etchant, volume %
GE-1541 NASA-15T NASA-15T2 Armco 18 SR NASA-18 T	10 H_2SO_4 + 90 H_2O (2g CrO_3)
AISI 651	40 HCl + 10 HNO_3 + 50 H_2O
AISI 310	10 H_2SO_4 + 90 H_2O (2g CrO_3)
Inconel 601	33 HNO_3 + 33 CH_3COOH + HF + 33 H_2O

The metallographic samples were taken from the reactor core locations noted in figure 1 by electrical discharge machining. Surfaces of the reactor cores were examined by X-ray diffraction, spectrographic, and electron microprobe techniques to identify oxide scales, surface chemistry, and the presence of foreign constituents.

Screening tests. - In the screening tests, the reactor test cores were examined after 12, 25, 50, 100, and 200 hours of testing. Uncoated alloys were considered to have failed if the core weight loss exceeded 5 percent. The nominal weight of the reactor test cores was 1000 to 1300 grams (2.2 to 2.9 lb) prior to test. Coated reactors were considered to have failed if the core weight loss exceeded the weight of the depos-

ited coating. In both cases, core penetration by a burnthrough or by oxidation and erosion was classified as a failure.

Reactor core distortion was determined at each inspection interval by measuring the change in core diameter. The core diameter at the point of maximum deformation (Dm) and the core diameter normal to that point (Dn) were used as a measure core distortion. The Dm and Dn values are given as percentages of the original core diameter. The maximum core distortion would be 40 percent (Dm) at which point the reactor core would contact the liner. In most cases Dn was less than the original core diameter and assigned a negative value.

Endurance tests. - Reactor performance in the endurance test was based on the same criteria as in the screening test except for the core weight loss of uncoated reactors. For the longer term tests, the core weight loss was used to compare the relative performance of the alloys evaluated. In addition, the bow of the reactor core, which was significant in the longer tests, was used as another measure of distortion. Bow was determined by measuring the deflection at the greatest point along the core length and was expressed as a percentage of core diameter. The maximum that a test reactor core could bow without touching the reactor liner was about 20 percent.

RESULTS

Preliminary Screening Tests - Uncoated Reactors

Reactor core weight change and distortion data obtained in the AC/C screening tests on uncoated reactors are presented in table V. The performance of the reactor materials is described in the following sections which are arranged by alloy class.

Ferritic-iron alloys. - Both ferritic-iron alloys GE-1541 and Armco 18 SR exhibited excellent oxidation resistance in the 200-hour test. For either alloy, the material loss (or gain) due to oxidation and/or erosion did not exceed 1 percent. The GE-1541 alloy exhibited the least distortion with only about a 5 percent maximum change in diameter. The Armco 18 SR reactor core had a maximum distortion of about 9 percent. Differences in reactor distortion are related to differences in high temperature strength. Although both alloys are relatively weak at high temperature, the GE-1541 alloy has about twice the strength of Armco 18 SR in stress rupture at 1000° C (1830° F) (see DISCUSSION section). Stresses applied to the reactor cores by the spring-loaded thermocouples (fig. 2) probably accounted for as much of the distortion as stresses induced thermally and by gas pressure.

Figure 6 shows the reactor cores of both ferritic alloys after the 200-hour tests. Both cores are in good condition. The missing support foot on the GE-1541 reactor in-

dicated a minor welding deficiency. Indentation of the Armco 18 SR core by the spring-loaded thermocouple is noted in figure 6. Photomicrographs of the reactor cores (fig. 7) showed only minor surface oxidation. Depletion of the second phase present in the GE-1541 alloy (YFe_9, ref. 9) occurred near the surface.

Based on their excellent performance in the screening test, both ferritic alloys were included in the reactor endurance testing phase of this program.

Austenitic-iron alloys. - The AISI 310 alloy core was not as oxidation resistant as the ferritic-iron alloys, but it only lost about 3 percent in weight in the 200-hour test. Resistance to distortion was very good with less than 1 percent change in reactor core diameter. Excessive oxidation of the AISI 651 alloy was observed in only 100 hours of testing. This test provided the baseline for evaluation of coated reactors since AISI 651 was used as the substrate for most of the coating evaluation studies. Since AISI 310 performed reasonably well in the screening tests and since it is one of the more oxidation-resistant austenitic alloys, it was selected for further evaluation in the reactor endurance testing phase of this program.

Nickel-base alloys. - The Hastelloy X reactor core exhibited excellent oxidation resistance and distortion resistance in the 200-hour test. However, the liner burned through as shown in figure 8. The localized penetration was probably caused by a hot spot although none was detected by the temperature probes. Metallographic analysis showed internal oxidation of the reactor core through grain boundaries to a depth of about 100 micrometers. Rather than Hastelloy X, the potentially lower cost Inconel 601 alloy was selected for inclusion in the endurance testing part of this program. In addition to lower cost, the Inconel 601 had shown better oxidation resistance in the thermal reactor environment than Hastelloy X in coupon screening tests of candidate reactor materials (ref. 8).

Preliminary Screening Tests - Coated Reactors

Test results for coated reactors subjected to the AC/C screening test are summarized in table VI. Performance of the coated reactors is presented in the following sections which are arranged by coating class. Reactor test cores and metallographic details are shown in figures 9 to 13.

Aluminide coatings. - For the Cr-Al coatings on AISI 651 and AISI 310 and the Al coating on Incoloy 800, the reactor test cores either gained or lost less than 1 percent in the 200-hour test. The weight change of these reactor cores was estimated to be less than 20 percent of the total amount of coating deposited. However, the central portion of the reactor cores showed evidence of coating degradation and localized penetration of the coating. Photomicrographs of the reactor core samples are shown in figure 9. As

shown, most of the coating is still present on the Cr-Al/AISI 651 and Al/Incoloy 800 sections with only minor substrate coating degradation. Coating penetration and substrate oxidation are evident for the Cr-Al/AISI 310 system. Overall, the Cr-Al/AISI 651 system was judged to have the least coating degradation. The only other major difference noted between these coatings was the wrinkling of the coating on Incoloy 800 (fig. 10(a)). This wrinkling had no apparent effect on the performance of the coating and the wrinkled areas remained intact.

Reactor core distortion was most severe for the Cr-Al/AISI 310 system with a 25 percent growth in core diameter (table VI). Probably most of this distortion was related to coating-substrate interactions and the thinner gage of the AISI 310. A Ni-Al layer probably formed at the coating substrate interface; this coating formation depleted nickel from the substrate. This resulted in the formation of a chromium-rich ferrite layer. Distortion would result from the stresses induced by the large difference in thermal expansion between the ferrite and austenite phases. Figure 10 shows the greater distortion of the Cr-Al/AISI 310 core in comparison to that of the Al/Incoloy 800, which had an 8 percent growth in diameter. The Cr-Al/AISI 651 system exhibited the least distortion. Thus, on the basis of overall performance, the Cr-Al/AISI 651 system was selected as the prime candidate for evaluation in the endurance testing phase of this program.

Glass-ceramic coatings. - The weight loss of the S-6100M/AISI 651 reactor core exceeded the coating failure criteria in about 150 hours of the AC/C test. The actual weight loss exceeded the as-deposited coating weight. In further testing to 200 hours the reactor core lost weight at approximately the same rate as uncoated AISI 651. As shown in figure 11, only an interdiffusion layer remained at the surface of the reactor core; this indicated that most of the protective coating was lost in the 200-hour exposure. The A418A/AISI 651 reactor core exhibited good oxidation resistance in the 200-hour test with less than 0.7 percent weight loss. The ceramic coating was still intact over the major portions of the core (fig. 12(b)). An interdiffusion layer, similar to that of the other ceramic core, was present in those areas depleted of coating as shown in the photomicrograph in figure 11.

In terms of distortion, the A418A AISI 651 reactor core exhibited very little dimensional change. Distortion of the S-6100M/AISI 651 reactor core was not more than 5 percent. Figure 12 shows the reactor cores after the 200-hour exposure. Both of the ceramic coated reactors showed evidence of local abrasion and loss of coating at sites of contact support (reactor port tubes, end pins, etc.). Further evaluation was considered to be warranted, however, since the ceramic coatings are potentially the least expensive of the coatings evaluated. The A418A/AISI 651 reactor was selected as a prime candidate for inclusion in the reactor endurance testing part of this program.

Slurry-metal coatings. - The Sermetal J/AISI 651 reactor core exceeded the coating failure criteria in less than 150 hours. In further testing to 200 hours the reactor core

lost weight at approximately the same rate as uncoated AISI 651. Reactor core deterioration was severe with a hole burn through between inlet ports (fig. 13(a)) and along a portion of the weld seam. Complete loss of coating was evident over most of the reactor core.

About one-third of the estimated coating deposited was lost in the 200-hour exposure of the NC-630/AISI 651 reactor core. General coating depletion and localized spalling was observed (fig. 13(b)). The NC-9/AISI 651 reactor core lost about 20 percent of the estimated coating deposited with a total loss in core weight of less than 1 percent. Localized areas of minor spallation and coating depletion were observed (fig. 13(c)). Metallographic evaluation of the reactor cores with the NC-630 and NC-9 coatings showed only minor degradation of the substrate even in areas where the coating was completely gone. The coating/substrate diffusion zones, probably rich in chromium, appeared to protect the substrate from severe oxidation.

Only minor core distortion was observed for the NC-630 and NC-9 coated reactors. The NC-9/AISI 651 reactor was judged to have the best overall performance, but both reactors were included in the endurance testing part of this program.

Endurance Tests - Uncoated Reactors

The uncoated alloys included in the endurance tests and the test results are summarized in table VII. Figure 14 shows the reactor core weight change data for most of the uncoated alloys as a function of test time. The results are presented for each material in the following sections which are arranged by alloy class.

Ferritic-iron alloys. - Two GE-1541 reactors were subjected to the endurance test cycle. The first reactor core exhibited localized failures along the weld seam after about 325 hours of testing. Testing was continued to a total of 650 hours to determine the performance of the unaffected core material. The extent of weld failure after 440 hours of exposure is shown in figure 15(a). After the 650-hour exposure, the reactor core lost less than 4 percent in weight and core distortion was minimal for the long term exposure with 5 percent growth in diameter and less than 3 percent bow. Other than the weld failure, the test core was in good condition as shown in figure 15(b). Similar weld corrosion was observed in the port tube weldments. Electron microprobe scans of the port tube weldments after 440 hours of exposure showed that the welds contained about 20 percent less chromium and about 25 percent less aluminum than the parent material. Thus, weldmetal depletion of these two elements during reactor fabrication was the likely cause for the weld failure noted in this test.

The modified weld alloy W-1, which contains larger amounts of chromium and aluminum, was used in fabricating the second GE-1541 reactor core. This reactor core

gave excellent performance in the endurance test. At the completion of the program, the W-1 welded core had been subjected to 684 hours of test exposure with less than 1 percent weight gain and no weld corrosion. Of the reactors tested, the GE-1541 showed the least core distortion, 4 percent change in diameter and 6 percent bow. Photographs of the reactor core after the endurance test exposure are shown in figures 15(c) and (d).

Metallographic sections of both of the GE-1541 reactors were very similar. Figure 16 shows a typical microstructure of the reactor exposed to 684 hours of testing. The structure is sound; it exhibits only minor surface damage to a depth of about one grain, and there is depletion of the second phase (YFe_9, ref. 9) in these areas. Freedom of the W-1 alloy weldment from corrosion is illustrated in figure 16(c) for the weldment of the thermocouple stud. Thermocouple studs welded with the GE-1541 filler rod corroded and fell off prior to completion of the 650-hour test exposure.

The protective oxide scale on the GE-1541 reactor core was identified as alumina by X-ray diffraction. Traces of yttria were also observed in the scale which was very adherent with no evidence of spallation. Similar results have been observed in static oxidation tests of this type of alloy (ref. 9).

Only one Armco 18 SR reactor was subjected to the endurance test. This reactor core failed by localized oxidation after 616 hours of exposure. Complete penetration of the core occurred on one end near the exhaust holes as shown in figure 17(a). Total core weight loss was less than 2 percent; this small weight loss indicated the localized nature of the core failure. Metallographic analysis of the failure area and of a similar area at the other end of the core indicated excessive localized oxidation but no evidence of melting. Other areas of the reactor core exhibited only minor surface oxidation which suggests the failure might have resulted from a hot-spot condition. However, none was indicated by the temperature probes.

Metallographic analysis of the reactor core showed the structure to be sound with only minor surface oxidation and oxide penetration into the substrate (figs. 18(a) and (b)). The protective oxide scale on the reactor core was adherent and was identified as a mixture of chromia and alumina with traces of silica and titania. Figure 19(a) shows a scanning electron photomicrograph of the mixed oxide scale and oxide penetration into the substrate near the surface.

Core distortion of the Armco 18 SR was considered excessive with up to a 17 percent change in diameter and a 10 percent bow (table VII). As noted in the screening tests, the spring-loaded thermocouples probably accounted for some of the core distortion. Thermocouple indentations were present in the Armco 18 SR core. Also, during the longer term endurance tests thermocouple binding in the reactor housing tended to apply a greater load on the reactor cores.

Modified ferritic-iron alloys. - Three modified ferritic-iron alloys were evaluated in the endurance test. They were NASA-18T, a tantalum (1.25 percent) modification of Armco 18 SR, and two tantalum modifications of the GE-1541 alloy, NASA-15T, and NASA-15T2. The latter modified alloys did not contain yttrium (see table I).

At the completion of the program the NASA-18T alloy had been exposed to the endurance test for 762 hours without failure. Core weight loss was less than 1 percent. However, core distortion was considered to be excessive. Overall core distortion was slightly greater than that of Armco 18 SR (table VII). The binding of the spring-loaded thermocouples was more severe during the testing of the NASA-18T alloy; this severe binding probably accounts for the greater core distortion of the NASA-18T alloy as compared to the Armco 18 SR alloy. Figure 17(b) shows the NASA-18T alloy core after the 762-hour test exposure.

A microstructural examination of the NASA-18T reactor core showed only minor surface oxidation with the structure remaining integrally sound (figs. 18(c) and (d)). The tightly adherent oxide scale on the NASA-18T reactor core was significantly different than that found on the Armco 18 SR reactor core as illustrated in the scanning electron photomicrographs of figure 19. A two-layer oxide scale was observed on the NASA-18T alloy which had a total thickness of about 13 μm (about 30 percent thinner than the scale on Armco 18 SR). The outer layer contained alumina and silica. A microprobe analysis showed that only aluminum was present in the inner layer; this indicated the presence of only alumina. A comparison of the photomicrographs in figures 18 and 19 indicates that the oxide scale on the NASA-18T alloy is more protective since oxide penetration into the substrate occurred only in the Armco 18 SR.

The reactors produced from the modified GE-1541 alloys, NASA-15T, and NASA-15T2, lasted less than 500 hours when being endurance tested (table VII). Failure by penetration through the core was observed for the NASA-15T2 alloy after 470 hours of testing. Excessive distortion was noted for both modifications when compared to the distortion of the GE-1541 alloy (table VII). The testing of the NASA-15T alloy was terminated after 404 hours of exposure with severe core distortion around the exhaust inlet and outlet holes. Although the total weight change of these reactor cores was less than 1 percent, both cores exhibited severe surface and internal oxidation as shown in figure 20.

Both modified alloys formed an alumina scale that appeared to be thicker than that found on the GE-1541 alloy. Oxide spalling was evident on both modified alloy cores. These results tend to support other work (ref. 9) with respect to the beneficial effects of yttrium in terms of providing a more adherent oxide scale and in terms of increasing the high temperature strength of this type of ferritic-iron alloy.

Austenitic-iron alloys. - AISI 310 was the only austenitic-iron alloy evaluated in the endurance test. The reactor core wall thickness was increased from the 1.22 milli-

meters (0.048 in.) used in the screening tests to 1.60 millimeters (0.067 in.) to help accommodate the high weight loss anticipated based on the screening test results. The AISI 310 reactor core failed in less than 500 hours with the core weight loss exceeding 20 percent. Testing was continued to 585 hours. After 585 hours of exposure the core was thinned and penetrated (as shown in fig. 21(a)) and the core weight loss was 35 percent. A metallographic analysis of the reactor core showed the failure to be by general oxidation and corrosion.

Nickel-base alloys. - Inconel 601 was the only nickel-base alloy subjected to the endurance test. Overall, this alloy performed well and was left on test until the completion of the test program. Total exposure was 1000 hours. Interim measurements made after about 650 hours of exposure indicated that core weight loss approached 5 percent, core distortion was 10 percent, and bow was about 15 percent (table VII). Also, minor thermal fatigue cracks (about 1.2 cm (0.5 in.) long) were observed around some of the exhaust outlet holes. A slight growth of the cracks was noted after 850 hours, which was the last inspection prior to the end of the test. After the 1000-hour exposure the core exhibited a 9 percent weight loss with 32 percent diametrical distortion, and no change in bow from the 650-hour measurement. Figure 21(b) shows the reactor core after the 1000-hour exposure. Extensive distortion and the fatigue cracks can be noted around the exhaust outlet holes. The port tube shown in figure 21(b) was flared inside the core.

Metallographic examination of the core showed extensive surface oxidation and internal oxidation to a depth of about one-third the material thickness (fig. 22).

Endurance Tests - Coated Reactors

The endurance test results for the coated reactors are summarized in table VIII. The performance of the coated reactors is presented by coating type in the following sections. No metallographic analysis of the coated reactors was made after endurance testing since they all failed after exposure times that did not greatly exceed the 200-hour screening tests. For most of the coated reactors the results indicated that the endurance test cycle was more severe than the screening test.

Aluminide coatings. - Reactor cores of Cr-Al/AISI 651 and Cr-Al/AISI 310 were subjected to the endurance test. The Cr-Al/AISI 651 core failed by penetration and severe deterioration in 325 hours of exposure. (The failure was similar to that shown in figure 23 for the NC-9/AISI 651 reactor core.) Excessive distortion of the Cr-Al/AISI 310 core occurred in only 65 hours of testing (table VIII). Since the distortion was nearly equal to that observed in the 200-hour screening test, no further testing was warranted.

Glass-ceramic coatings. - The A418A/AISI 651 coating system was evaluated in the endurance test. Failure of the reactor core occurred by general coating depletion after only 162 hours of exposure. Reactor core weight loss exceeded 11 percent (table VIII).

Slurry-metal coatings. - The NC-9/AISI 651 and the NC-630/AISI 651 slurry metal coated systems were evaluated in the endurance test. Complete failure by penetration and deterioration of the NC-9/AISI 651 reactor core occurred in less than 325 hours of exposure (fig. 23). Core weight loss exceeded 30 percent. Endurance testing of the NC-630/AISI 651 reactor core was discontinued after 228 hours of exposure. Although the reactor core weight loss was only 8 percent, the core showed nearly complete loss of coating, thinning around the exhaust holes, and evidence of thermal cracking in these areas.

Effects of Fuel Composition

Lead, phosphorus, and calcium were detected at varying trace levels on the surfaces of most of the reactor components tested in both leaded and unleaded fuel. Calcium, which probably came from the engine oil, was usually present in the form of calcium phosphate on the reactor material surfaces.

Of the materials evaluated in this study, only AISI 310 exhibited a direct relation between fuel composition and performance in the reactor tests. Reactor port tubes of several alloys were replaced with unexposed port tubes in the endurance test to provide total exposure to either leaded or unleaded fuel. As shown in table IX, AISI 310 exhibited a greater weight loss when exposed to unleaded fuel. Other alloys, such as GE-1541 and Inconel 601, showed only minor changes in port tube weight loss or gain when exposed to leaded or unleaded fuel. No specific cause was determined for the behavior of AISI 310 in this test.

Since the endurance tests of coated reactors were conducted using leaded fuel, an additional test was made using unleaded fuel. Because of their availability, a S6100 M ceramic coated reactor and a Sermetel J metallic coated reactor were selected for this test. To decrease the test severity, the peak cycle temperature was reduced to 980^{o} C (1800^{o} F). Both reactors failed in less than the 228-hour exposure. Core weight losses exceeded 10 percent (table VIII), the coatings were completely gone, and the cores were penetrated near the exhaust outlet holes. Overall, these reactors were degraded more severely than similar reactors subjected to the 200-hour screening test using leaded fuel and a higher peak cycle temperature. Like most of the other coated reactor test results, these results indicate the greater severity of the endurance test cycle even with a reduced peak cycle temperature. They also indicate that leaded fuel was not a major factor in the degradation of coated reactors.

Test engine life using leaded fuel in the endurance test was about 1000 hours. Most of the deterioration was associated with the valves, valve seats, and stems with no severe wear of the pistons and cylinder walls. With unleaded fuel and hardened valve seats engine life was about 1200 hours. Engine component degradation was similar to that observed when using leaded fuel.

DISCUSSION

Ferritic-Iron Alloys

Based on resistance to oxidation, erosion, and distortion, the GE-1541 alloy exhibited the best performance of all the materials evaluated in this program. Based on performance alone, this alloy would be an excellent candidate for thermal reactor use. Reactor cores of this alloy performed extremely well in the nearly 700-hour exposure provided in this evaluation. Longer tests were not conducted on this alloy due to the termination of the program. Since the engines lasted only 1000 to 1200 hours under the endurance test conditions, the 700-hour tests represent a reactor life of at least 60 to 70 percent of engine life.

The NASA-18T alloy is also considered to be a good candidate for thermal reactor use. It provided excellent resistance to oxidation and corrosion in the endurance test, but its distortion was excessive. In 1000° C (1830° F) stress-rupture tests the NASA-18T alloy has about 10 percent less strength for a 100-hour life than the GE-1541 alloy (fig. 24). We believe the thermocouple binding problem aggravated the distortion and precluded demonstrating the advantage of this alloy, particularly when compared to Armco 18 SR. As shown in figure 24, the stress for a 100-hour life at 1000° C (1830° F) is about 50 percent higher for the modified alloy than for Armco 18 SR. A comparison of reactor liner distortion did show that the NASA-18T alloy had less bow after a 500-hour exposure than the Armco 18 SR liners had after only a 260-hour exposure. Even with the 20 percent core distortion of the NASA-18T alloy it is unlikely that reactor performance would have been affected with the reactor design used in this study since about 40 percent distortion would be required to effectively block exhaust gas passages.

Armco 18 SR performed reasonably well in the endurance tests, and it also would be a good candidate material for reactor use. Another thermal reactor test of this alloy (ref. 12) indicated its potential for reactor use. Because that test was less severe in terms of peak temperature and cyclic operation a direct comparison with the results obtained in our evaluation was not possible. However, localized oxidation failure of Armco 18 SR was observed in related coupon tests (ref. 12) as a result of local breakdown ("warting") of the aluminum-rich oxide scale with subsequent formation of an iron-rich scale which enhanced oxidation attack. A similar breakdown in the protective oxide

scale appears to have caused the severe localized oxidation and core penetration noted in the endurance tests of Armco 18 SR. An oxidation failure of this type may not occur with the NASA-18T alloy since the protective oxide scale is appreciably different. The oxide scale on Armco 18 SR, after exposure to the endurance test was a mixture of alumina and chromia. A thinner and apparently more adherent two layer oxide scale containing primarily alumina protects the NASA-18T alloy. Similar differences in oxide scales were observed in cyclic furnace oxidation tests of these alloys (unpublished data obtained by the authors).

Nickel-Base Alloys

Inconel 601 performed well in the endurance test, which lasted nearly the life of the test engine. Oxidation and distortion were extensive after the 1000-hour exposure, but the reactor core remained intact. On a performance basis, this higher cost alloy would be a good candidate for thermal reactor use. It has shown good resistance to the reactor environment in coupon tests (refs. 4, 8, and 12) and in vehicle tests of full-size reactors (ref. 1). Other full-size reactor tests were not as severe as the endurance test used in this evaluation so a direct comparison cannot be made.

Coatings

The relative short life of the coated reactors and the higher cost of a coated reactor system would appear to eliminate them from further consideration, particularly since the the low cost uncoated alloys are more resistant to the thermal reactor environment. Other tests of coatings have shown them to be beneficial in providing longer life reactor materials (refs. 3, 4, and 12). However, those tests were not as severe as the endurance test used in this study in terms of the combined peak temperature and cyclic operation.

Fuel Composition

With respect to fuel constituents, more comprehensive studies have been conducted relating fuel composition to thermal reactor materials behavior (refs. 4 and 12). In one case, leaded fuel was shown to cause greater corrosion of AISI 310. The other study did not show any appreciable difference between leaded and unleaded fuel on the performance of AISI 310. Our results indicated unleaded fuel to be more detrimental for AISI 310. In all cases, Inconel 601 appeared to be relatively insensitive to changes from leaded to un-

leaded fuel. The differences in the performance of AISI 310 is probably related to other fuel constituents, such as phosphorus, sulphur, and halides, acting independently or in conjunction with lead. In selected cases where other fuel constituents have been varied along with the lead content significant changes in material performance have been observed (refs. 4 and 12).

Materials for Reactor Use

When considering the ferritic-iron alloys for reactor use we would give preference to the Armco 18 SR and NASA-18T alloys over GE-1541 because of their better fabricability. Warm forming, which is required for the GE-1541 alloy, appears to be a major deterrent to its use. Armco 18 SR has reasonably good fabricability at ambient temperature (ref. 10). Fabricability of the NASA-18T alloy is similar to Armco 18 SR in terms of sheet manufacture, Olsen cup tests, bend tests, and tensile elongation (unpublished data obtained from D. L. Chalk, Armco Steel Corporation). Also, the fabricability of the two alloys was judged to be similar in the manufacture of the test reactor components. The NASA-18T alloy offers increased high-temperature strength and oxidation resistance as compared to Armco 18 SR but at a higher material cost due to the tantalum addition. This cost difference could be as high as 40 percent. Because of the yttrium content and the greater difficulty in sheet manufacture, it is likely that the cost of the GE-1541 alloy would be higher than that of the NASA-18T alloy.

The high cost of Inconel 601 (at least twice that of the ferritic-iron alloys) and its high nickel content would be the principal factors limiting its use in thermal reactor applications. However, for reactor designs that require a higher strength alloy the use of Inconel 601 would be warranted.

Since reactor design can significantly influence materials selection, these material preferences might be altered for reactor designs appreciably different from the design evaluated in this study. A reactor designed for actual use might be appreciably different due to emission or vehicle compatibility requirements. For example, thin gage sheet material might be required to reduce reactor thermal inertia to provide adequate emission control from a cold start. From this aspect, the ferritic-iron alloys may not have adequate strength if material thickness requirements were of the order of 0.07 centimeter (0.03 in.).

CONCLUSIONS

Of the alloys and coatings evaluated in this study, the ferritic-iron alloys GE-1541, Armco 18 SR, and NASA-18T and the nickel-base alloy Inconel 601 should be considered

for future reactor use. On the basis of low cost and fabricability, preference should be given to the Armco 18 SR and the NASA-18T alloys. The best overall performance was exhibited by the GE-1541 alloy. However, the poorer fabricability of this alloy is probably a major deterrent to its use. The use of Inconel 601, which is more costly than the ferritic-iron alloys, might be warranted for reactor designs that require a higher strength alloy.

None of the coating systems evaluated warrant consideration for reactor use. Performance of the coatings was very poor, and the coating systems evaluated would be more costly than the uncoated ferritic-iron alloys.

Reactor design, which can greatly influence material selection, was not evaluated in this study in terms of emission performance or vehicle compatibility. Thus, reactor designs significantly different than the one evaluated in this report might be required in actual use. A major change in design might alter the previous material preferences.

Lewis Research Center,
National Aeronautics and Space Administration,
Cleveland, Ohio, March 11, 1974,
501-21.

REFERENCES

1. Campau, R. M.: Low Emission Concept Vehicles. Paper 710294, SAE, Jan. 1971.
2. Cantwell, E. N.; and Pahnke, A. J.: Design Factors Affecting the Performance of Exhaust Manifold Reactors. Paper 650527, SAE, May 1965.
3. Cantwell, E. N.; Rosenlund, I. T.; Barth, W. J.; Kinnear, F. L.; and Ross, S. W.: A Progress Report on the Development of Exhaust Manifold Reactors. Paper 690139, SAE, Jan. 1969.
4. Jaimee, A.; Schneider, D. E.; Rozmanith, A. I.; and Sjoberg, J. W.: Thermal Reactor-Design, Development, and Performance. Paper 710293, SAE, Jan. 1971.
5. Lang, Robert L.: A Well-Mixed Thermal Reactor System for Automotive Emission Control. Paper 710608, SAE, June 1971.
6. Oldrieve, Robert E.; and Saunders, Neal T.: Materials Problems in Automobile Exhaust Reactors for Pollution Control. Aerospace Structural Materials. NASA SP-227, 1970, pp. 317-330.
7. Blankenship, Charles P.; and Hibbard, Robert R.: NASA-EPA Automotive Thermal Reactor Technology Program, Status Report. NASA TM X-68010, 1972.

8. Oldrieve, Robert E.: Exploratory Screening Tests of Several Alloys and Coatings for Automobile Thermal Reactors. NASA TM X-67984, 1971.

9. Wukusick, C. S.: The Physical Metallurgy and Oxidation Behavior of Fe-Cr-Al-Y Alloys. GEMP-414, Nuclear Technology Dept. General Electric Co., June 1, 1966.

10. Anon.: Armco 18 SR Stainless Steel Sheet and Strip. Product Data Report S-47b, Advanced Materials Division, Armco Steel Corp., 1972.

11. Stone, Philip L.; and Blankenship, Charles P.: Exploratory Evaluation of Ceramics for Automobile Thermal Reactors. Paper 730224, SAE, Jan. 1973.

12. Barth, W. J.; and Cantwell, E. N.: Automotive Exhaust Manifold Reactors-Materials Considerations. Paper presented at the 161st Meeting, American Chemical Society (Los Angeles, Calif.), Mar. 28-Apr. 2, 1971.

TABLE I. - COMPOSITIONS OF ALLOYS EVALUATED

Alloy designation	Sheet gage		Alloying elements, wt %											Alloy vendor
	mm	(in.)	Fe	Cr	Ni	Mo	W	Ti	Al	C	Mn	Si	Other	
GE-1541	1.60	(0.063)	Balance	14.5	0.03	---	----	----	4.5	0.002	-----	----	1.0 Y	General Electric Co.
NASA-15T[a]	1.58	(.062)	↓	14.7	----	---	----	----	4.3	.01	0.001	0.05	.9 Ta	General Electric Co.
NASA-15T2[a]	1.58	(.062)		15.2	----	---	----	----	5.4	.01	.001	.05	2.0 Ta	General Electric Co.
Armco 18 SR	1.75	(.069)		18.0	.50	---	----	0.40	2.0	.05	.50	1.0		Armco Steel Co.
NASA-18T[a]	1.55	(.061)		17.8	.50	---	----	.45	2.1	.04	.37	1.28	1.25 Ta	Armco Steel Co.
AISI 651[b]	1.65	(.065)		18.5	9.0	1.4	1.35	.25	---	.32	1.15	.6	.4 (Cb + Ta)	Several
AISI 310[c]	1.22	(.048)		25.0	20.0	---	----	----	---	.25	2.0	1.5	---	Several
Incoloy 800[b]	1.37	(.054)	46	20.5	32	---	----	.4	.4	.04	-----	----	---	International Nickel Co.
Hastelloy X	1.25	(.049)	18.5	21.8	Balance	9.0	.6	----	---	.10	1.0	.5	1.5 Co	Cabot Corp.
Inconel 601	1.30	(.051)	14.1	23	60.5	---	----	----	1.35	.05	.5	.25	---	International Nickel Co.

[a]Denotes actual compositions, others are nominal.

[b]Used as a substrate for coating evaluation.

[c]Also evaluated in 1.70-mm (0.067-in.) gage.

TABLE II. - COATING SYSTEMS EVALUATED

Coating systems		Coating	Application method		Amount deposited on reactor core,[a] mg/cm^2	Coating vendor (coating trade name)
Key	Substrate		Liner	Core		
Cr-Al	AISI 651	Cr-Al	Pack	Pack	10	Alloy surfaces (HI-15)
Cr-Al	AISI 310	Cr-Al	Pack	Pack	17	Alloy surfaces (HI-15)
Sermetel J	AISI 651	Al	Spray	Dip	2	Teleflex (Sermetel J)
Al	Incoloy 800	Al	Pack	Pack	20	Alloy surfaces (HI-15-12)
S-6100 M	AISI 651	Ceramic	Spray	Dip	7	Wall Colmonoy (Solaramic 6100M)
A-418A	AISI 651	Ceramic	Spray	Dip	3	Lycoming (NBS A-418A)
NC-9	AISI 651	Ni-Cr	Spray	Spray	28	Wall Colmonoy (Nicrocoat 9)
NC-630	AISI 651	Ni-Cr	Spray	Spray	66	Wall Colmonoy (Nicrocoat 630)

[a]Based on weight gain.

TABLE III. - ENGINE PARAMETERS FOR ACCELERATED CREEP AND CORROSION TEST CYCLE

Engine parameter	Test cycle condition	
	Peak temperature	Idle
Rotational speed, rpm	3200	800
Dynamometer load, m-N (ft-lb)	150 (111)	0
Ignition timing	6° retarded	6° retarded
Fuel flow, kg/hr (lb/hr)	23 to 25 (50 to 55)	3 (7)
Manifold vacuum, kN/m^2 (in. Hg)	37 to 40 (11 to 12)	57 (17)
Reactor annulus pressure, kN/m^2 (in. H_2O)	1.5 to 2.5 (6 to 10)	0.5 to 0.8 (2 to 3)

TABLE IV. - ENGINE PARAMETERS FOR ENDURANCE TEST CYCLE

Parameter	Simulated vehicle speed, km/hr (mph)		
	56 (35)	112 (70)	112 (70) with 900 kg (2000 lb) trailer
Rotational speed, rpm	1540	3030	3030
Dynamometer load, m-N (ft-lb)	48 (35)	92 (68)	255 (188)
Ignition timing	6° retarded	6° retarded	6° retarded
Fuel flow, kg/hr (lb/hr)	7 to 8 (16 to 18)	15 to 16 (34 to 36)	27 to 29 (60 to 64)
Manifold vacuum, kN/m^2 (in. Hg)	61 (18)	53 (16)	17 (5)
Reactor annulus pressure, kN/m^2 (in. H_2O)	0.3 to 0.5 (1 to 2)	1 to 2 (4 to 8)	3 to 5 (12 to 18)
Peak reactor temperature, $^{\circ}C$ ($^{\circ}F$)	840 (1550)	1050 (1925)	1040 (1900)

TABLE V. - SUMMARY OF THERMAL REACTOR SCREENING TEST

DATA FOR UNCOATED REACTORS

Reactor core material	After 200-hr exposure[a]			Remarks
	Weight change, percent	Length change, percent	Distortion,[b] percent, Dm, Dn	
GE-1541	0.48	0.30	5, -0	---
Armco 18 SR	-.68	.13	9, -5	Core distortion
AISI 310	-3.0	.26	None	---
AISI 651[c]	-6.3	----	----	Excessive weight loss
Hastelloy X	.45	-.10	None	Liner penetrated

[a]Test cycle: 2 hr at 1040° C (1900° F), forced air cooled to <70° C (<150° F), return to 1040° C (1900° F) each cycle for a total of 80 cycles.

[b]Maximum increase in core diameter, Dm; normal to Dm, Dn.

[c]Data for 100-hr exposure; test terminated due to excessive oxidation.

TABLE VI. - SUMMARY OF THERMAL REACTOR SCREENING

TEST DATA FOR COATED REACTORS

Reactor core, coating/substrate	After 200-hr exposure[a]			Remarks
	Weight change, percent	Length change, percent	Distortion,[b] percent, Dm, Dn	
Cr-Al/AISI 651	-0.26	2.9	5, -0	---
Cr-Al/AISI 310	.40	7.3	25, -0	Excessive distortion
Al/Incoloy 800	-.24	2.7	8, -3	Coating wrinkled
S-6100M/AISI 651	-8.30	.1	3, -5	Coating failure
A-418A/AISI 651	-.61	.3	None	---
NC-9/AISI 651	-.64	.2	None	---
NC-630/AISI 651	-2.36	.3	None	---
Sermetel J/AISI 651	-9.27	.8	----	Core penetrated

[a]Test cycle: 2 hr at 1040° C (1900° F), forced air cooled to <70° C (<150° F), return to 1040° C (1900° F) each cycle for total of 80 cycles.

[b]Maximum increase in core diameter, Dm; normal to Dm, Dn.

TABLE VII. - SUMMARY OF THERMAL REACTOR ENDURANCE TEST

DATA FOR UNCOATED REACTORS

Reactor core	Exposure time, hr	Percent of test time with leaded fuel	Length change, percent	Weight change, percent	Distortion, percent		Remarks
					Dm, Dn (a)	Bow	
GE-1541	650	68	0.2	-3.6	5, -0	2	Weld failure
GE-1541[b]	684	0	-.6	.3	3, -4	6	Excellent performance, W-1 weld rod
NASA-15T	404	0	.1	.6	14, -12	6	Localized oxidation failure
NASA-15T2	470	0	.4	-.1	12, -7	4	Core penetrated
Armco 18 SR	616	21	.7	-1.5	14, -17	10	Core penetrated
NASA-18T[b]	762	0	1.4	-.3	19, -23	6	Good performance, except for distortion
AISI 310	585	78	.2	-35	------	--	Failed by oxidation
Inconel 601[b]	650	80	.2	-4.5	10, -9	15	Minor fatigue cracks - test continued
	1000	45	1.4	-9.0	32, -14	15	Good performance for exposure time

[a]Maximum increase in core diameter, Dm; normal to Dm, Dn.

[b]Test terminated at end of program.

TABLE VIII. - SUMMARY OF THERMAL REACTOR ENDURANCE TEST DATA FOR COATED REACTORS

Reactor coating	Exposure time, hr	Percent of test time with leaded fuel	Weight change, percent	Length change, percent	Distortion,[a] percent, Dm, Dn	Remarks
Cr-Al	325	100	-16.5	1.9	---	Coating failure/core penetration
Cr-Al[b]	65	↓	.4	.9	9, -11	Excessive distortion
A418A	162		-11.5	1.9	---	Coating failure
NC-9	325		-31.0	.1	---	Coating failure/core penetration
NC-630	228		-8.3	.3	---	Coating failure
S6100M	228	0	-15.5	.6	19, -1	Coating failure/core penetration
Sermetel J[c]	228	0	-11.2	.7	12, -0	Coating failure/core penetration

[a]Maximum increase in core diameter, Dm; normal to Dm, Dn.
[b]AISI 310 substrate, all others AISI 651.
[c]Peak core temperature, 980° C (1800° F).

TABLE IX. - SUMMARY OF REACTOR PORT TUBE WEIGHT CHANGE DATA AFTER ENDURANCE TEST EXPOSURE TO LEADED AND UNLEADED FUEL

Alloy	Port tube weight change,[a] mg/cm^2			
	200-hr exposure		440-hr exposure	
	Leaded fuel	Unleaded fuel	Leaded fuel	Unleaded fuel
GE-1541	0.8	2.5	-3.85	2.80
AISI 310	-4.0	-20.0	-46	[b]-60
Inconel 601	2.5	4.3	1.2	0.4

[a]Average of three port tubes.
[b]Exposed for only 255 hr.

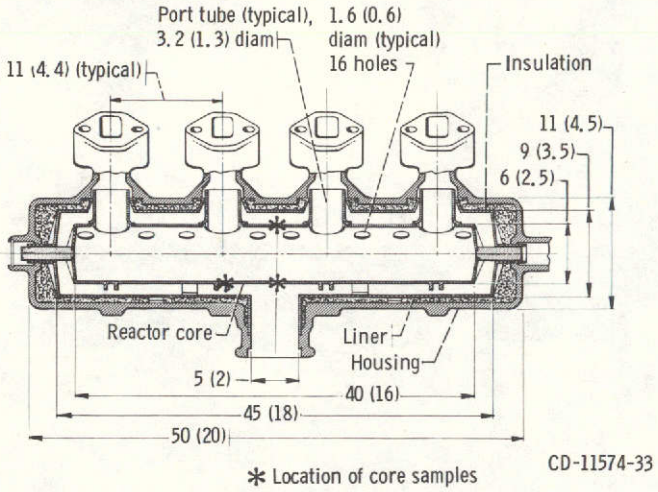

Figure 1. - Thermal reactor design for materials evaluation. All dimensions are in centimeters (in.).

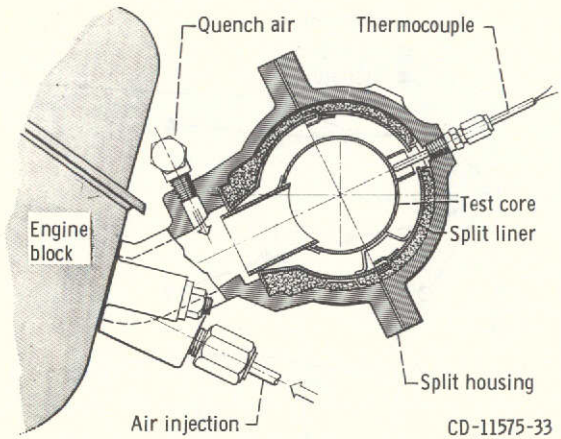

Figure 2. - Schematic of test reactor mounted on engine.

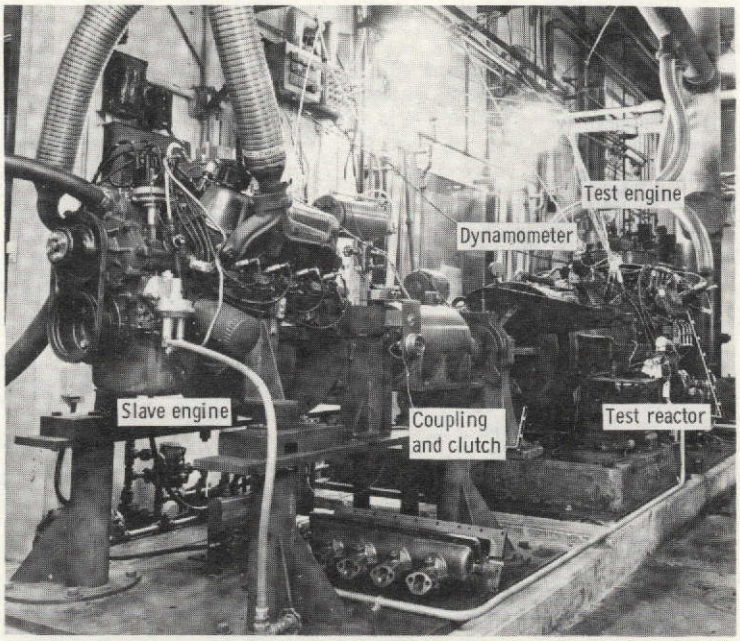

Figure 3. - Typical engine-dynamometer test stand installation.

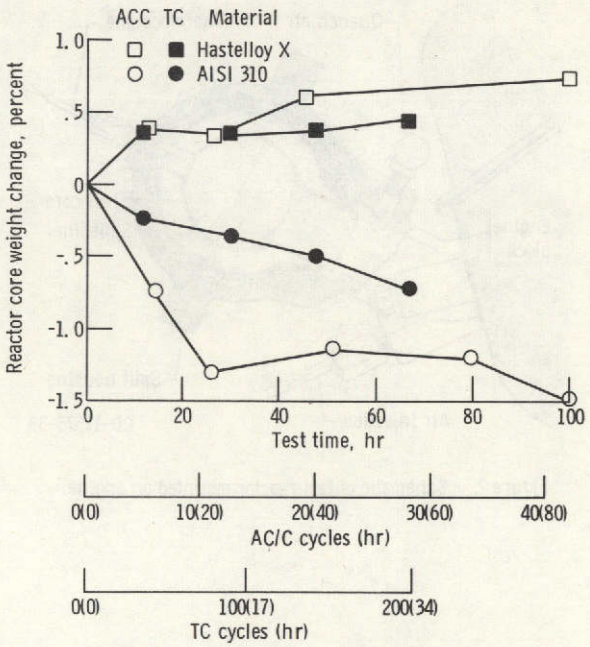

Figure 4. - Comparison of materials performance in accelerated creep and corrosion (AC/C) and thermal cyclic (TC) screening tests. Numbers in parentheses indicate hours at peak temperature.

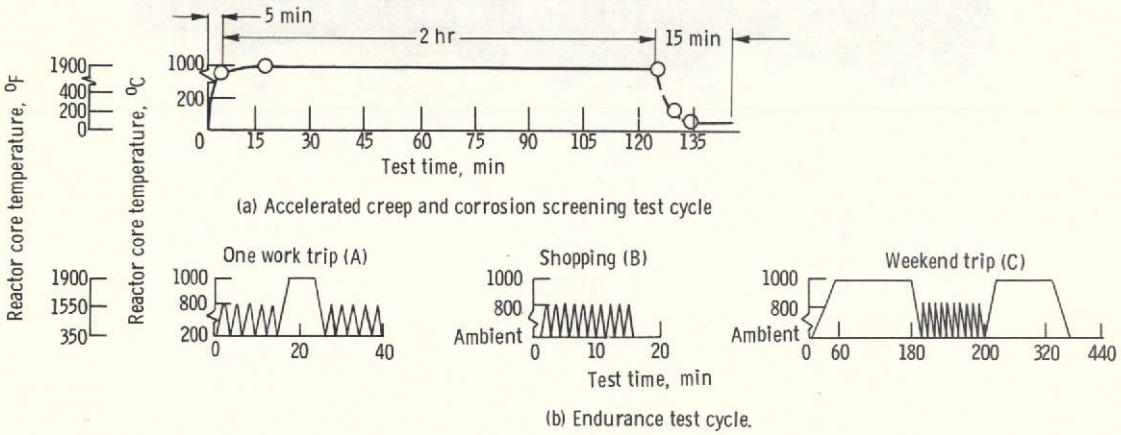

(a) Accelerated creep and corrosion screening test cycle

(b) Endurance test cycle.

Figure 5. - Thermal reactor screening and endurance test cycles.

(a) GE-1541 reactor core. X1.

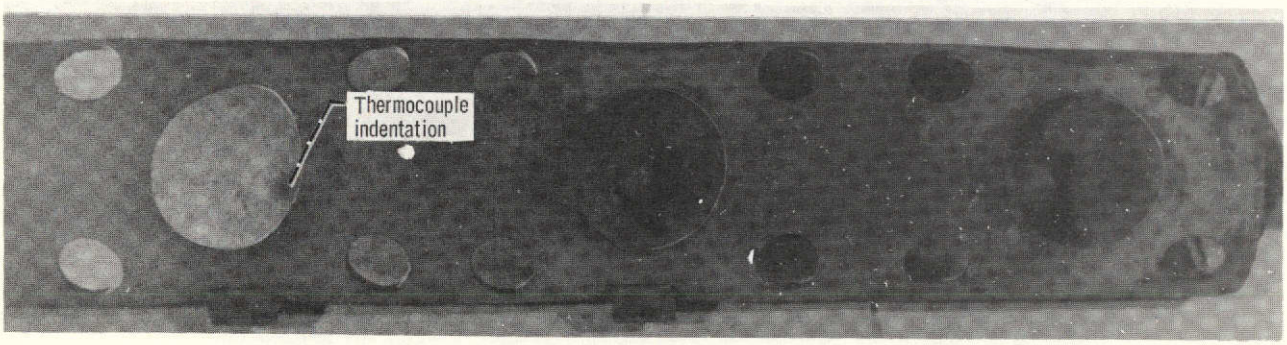

(b) Armco 18 SR reactor core. X1.

Figure 6. - Ferritic-iron-alloy reactor cores of GE-1541 and Armco 18 SR after exposure to 200-hour screening test.

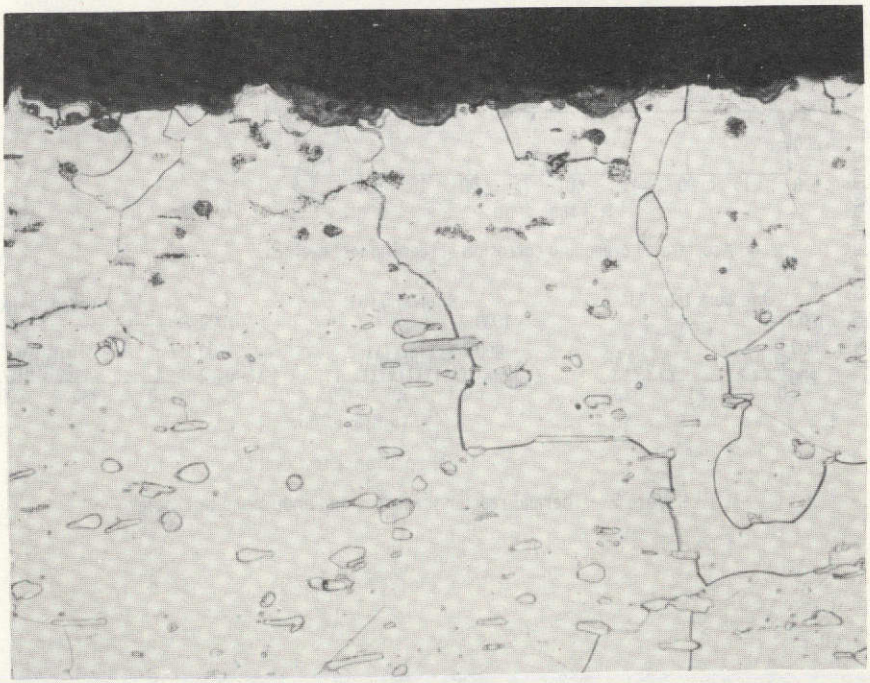

(a) GE-1541.

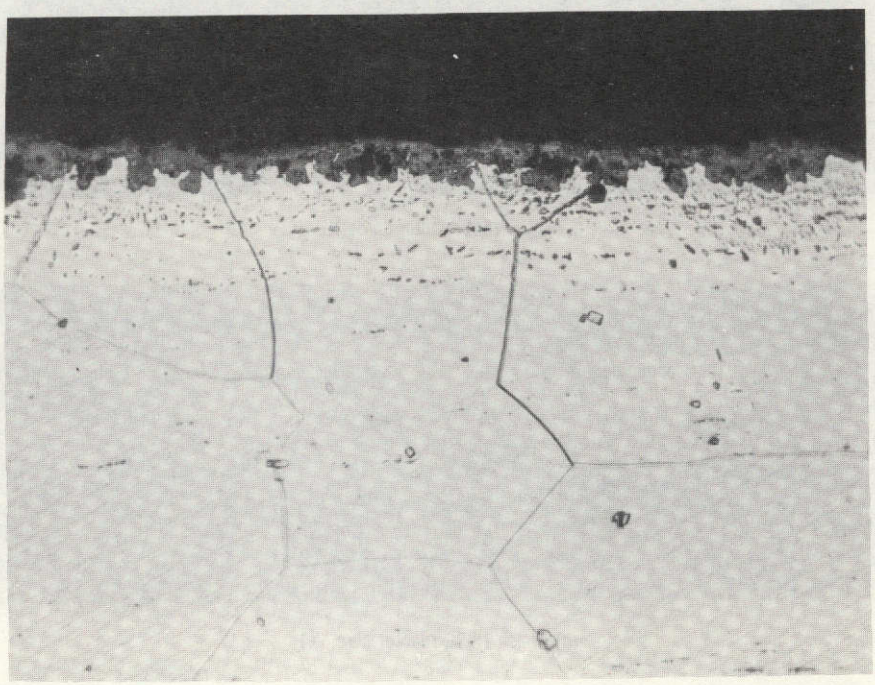

(b) Armco 18 SR.

Figure 7. - Photomicrographs of GE-1541 and Armco 18 SR reactor cores after exposure to 200-hour screening test. X250.

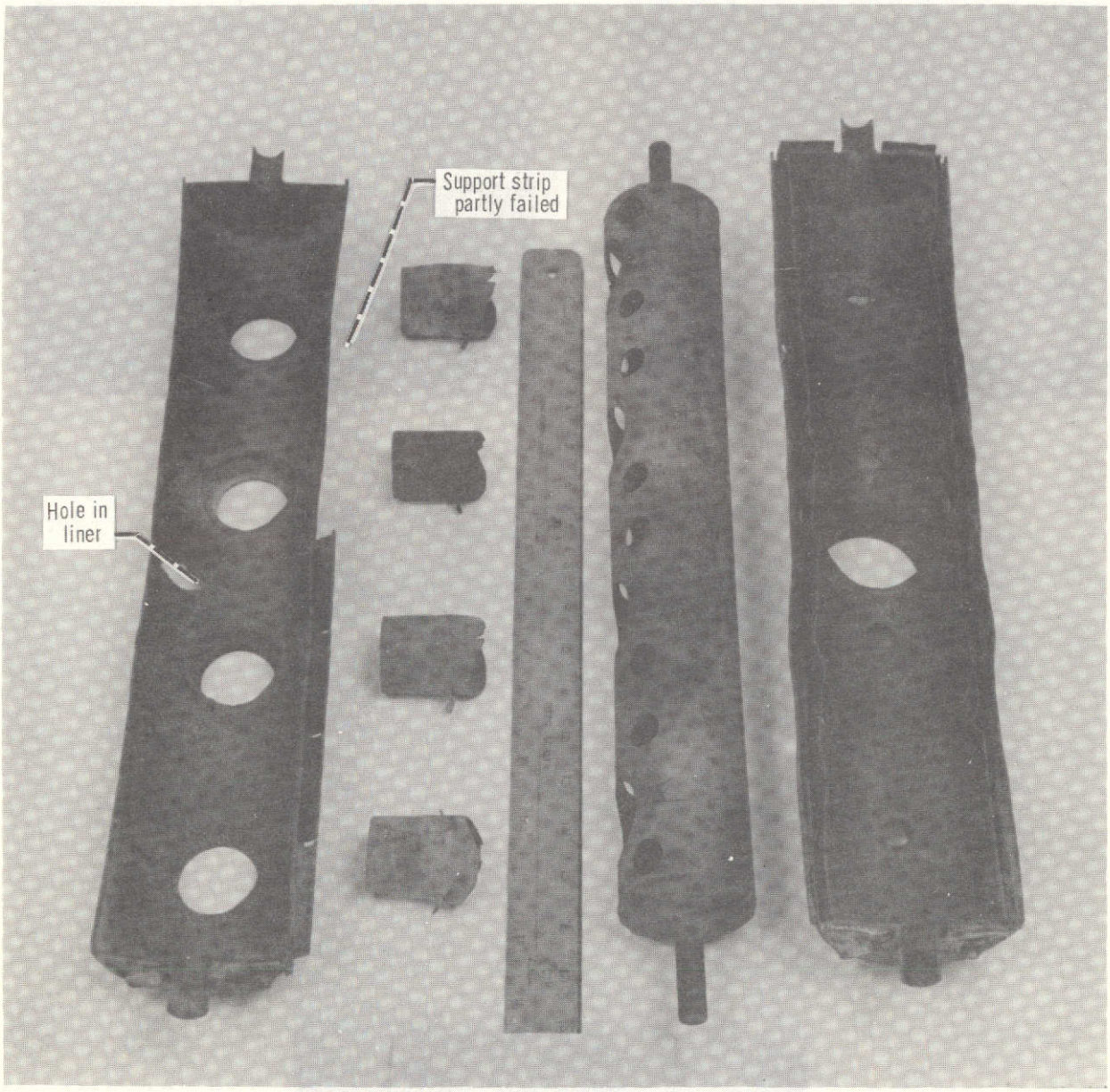

Figure 8. - Hastelloy X reactor components after exposure to 200-hour screening test.

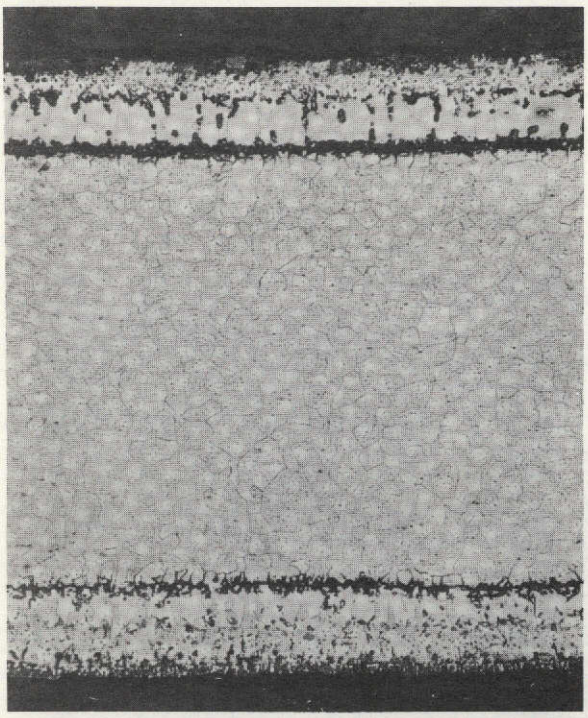

(a) Cr-Al/AISI 651.

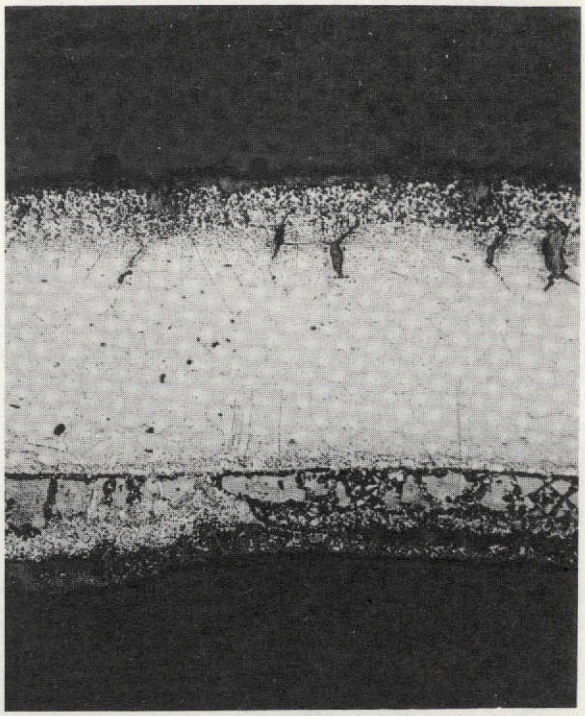

(b) Cr-Al/AISI 310.

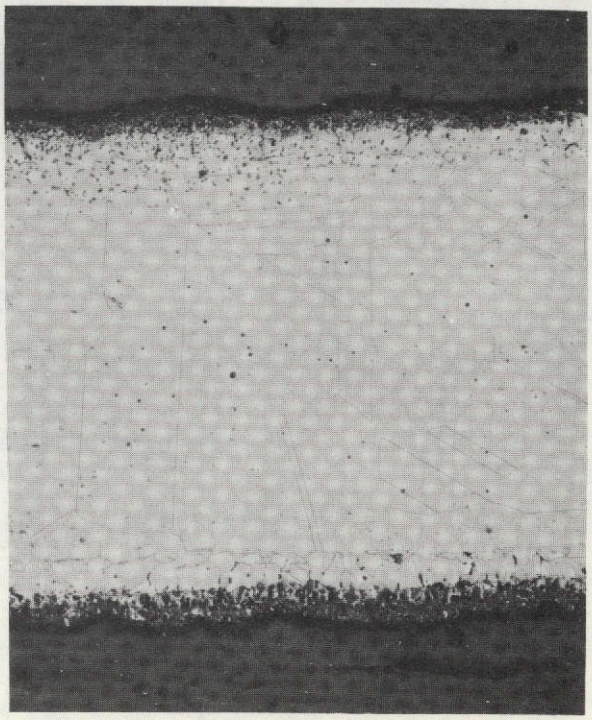

(c) Al/Incoloy 800.

Figure 9. - Photomicrographs of Cr-Al and Al coated reactor cores after exposure to 200-hour screening test. X50.

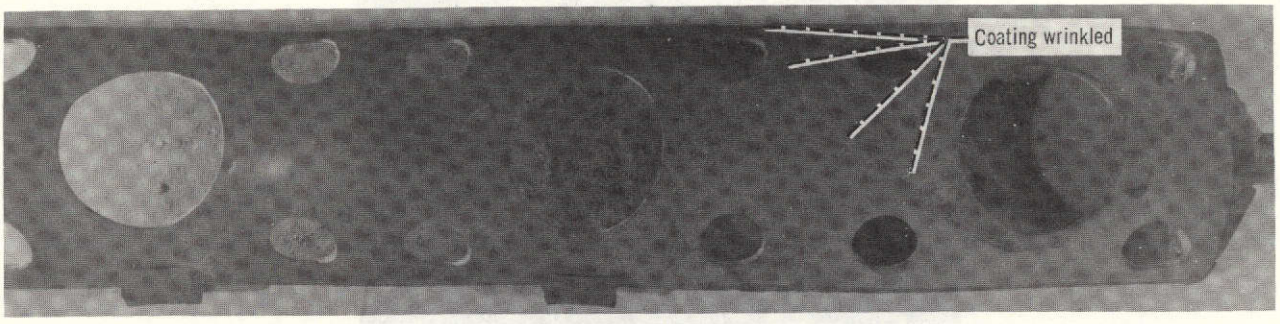

(a) Al coated Incoloy 800. X1.

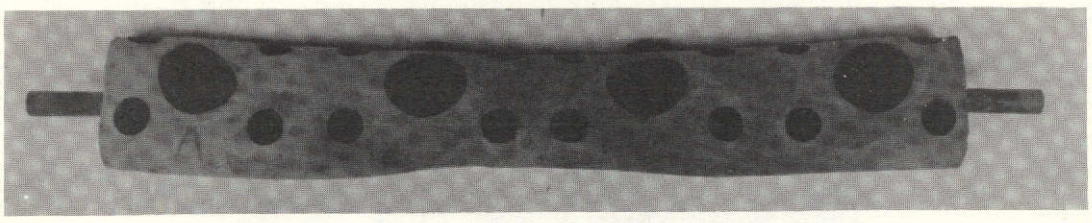

(b) Cr-Al coated AISI 310. X1/3.

Figure 10. - Al coated Incoloy 800 and Cr-Al coated AISI 310 reactor cores after exposure to 200-hour screening test.

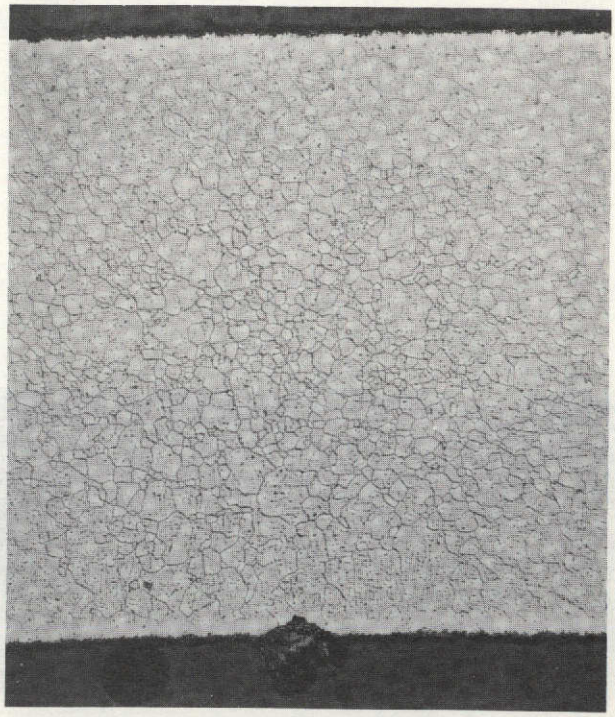

(a) S-6100M/AISI 651.

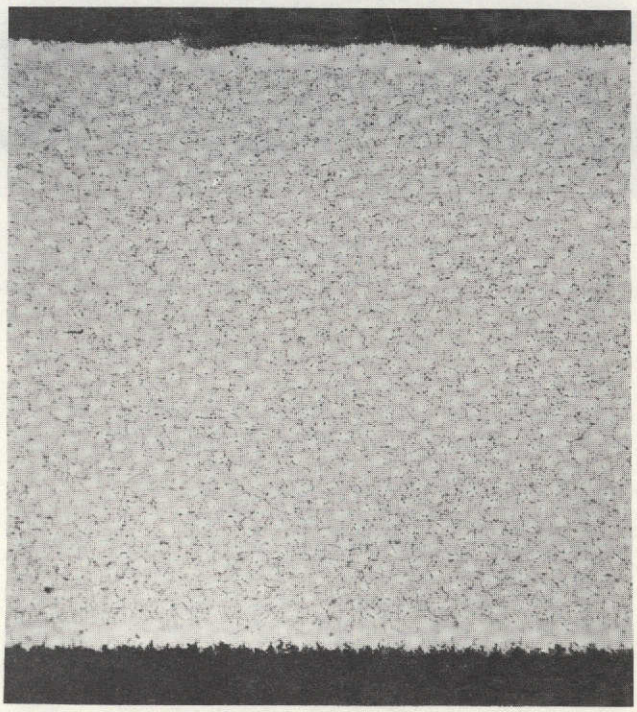

(b) A418A/AISI 651.

Figure 11. - Photomicrographs of S-6100M and A418A of ceramic coated AISI 651 reactor cores after exposure to 200-hour screening test. X50.

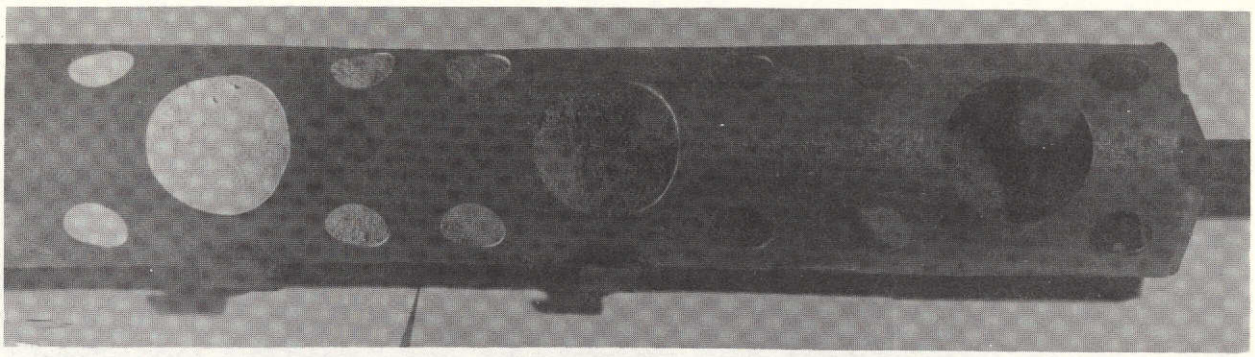

(a) S-6100M coated AISI 651.

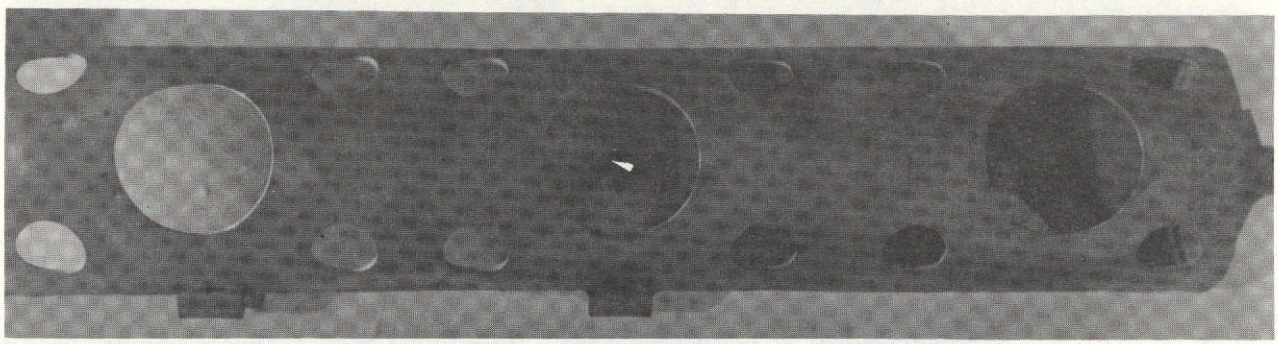

(b) A418A coated AISI 651.

Figure 12. - Glass-ceramic types S-6100M and A418A coated AISI 651 reactor cores after exposure to 200-hour screening test. X1.

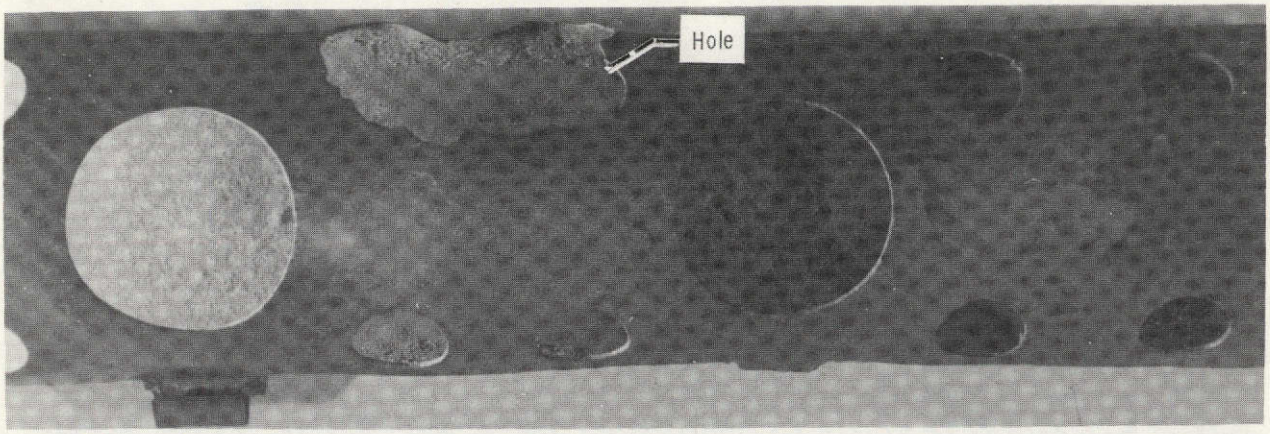

(a) Sermetel J coated AISI 651.

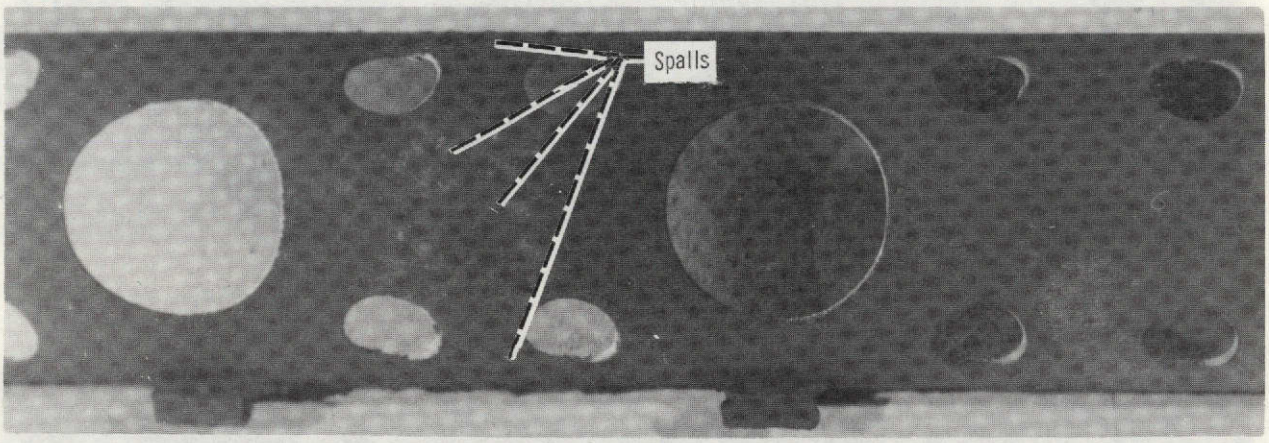

(b) NC-630 coated AISI 651.

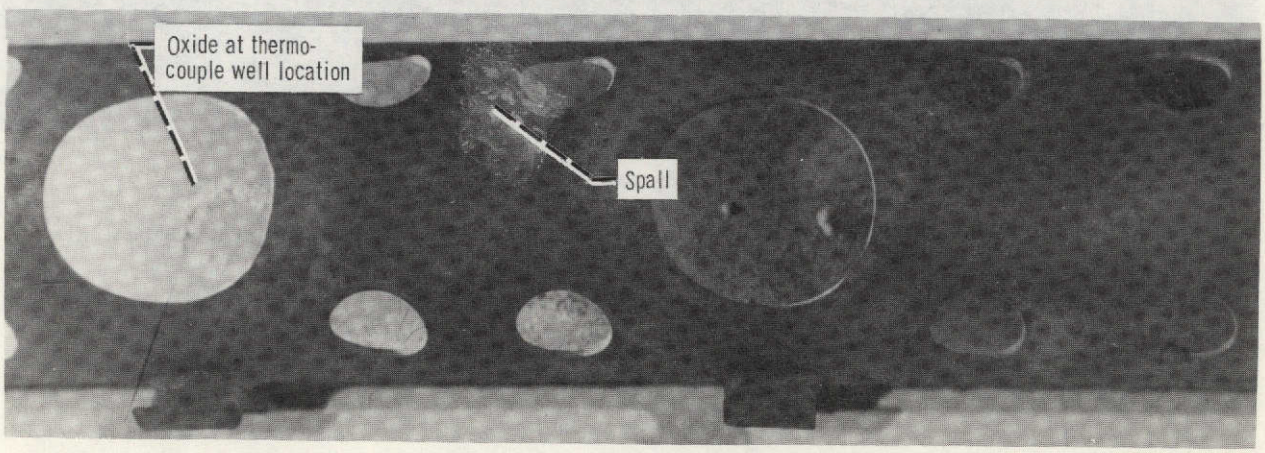

(c) NC-9 coated AISI 651.

Figure 13. - Slurry metal types Sermetel J, NC-630, and NC-9 coated AISI 651 reactor cores after exposure to 200-hour screening test. X1.

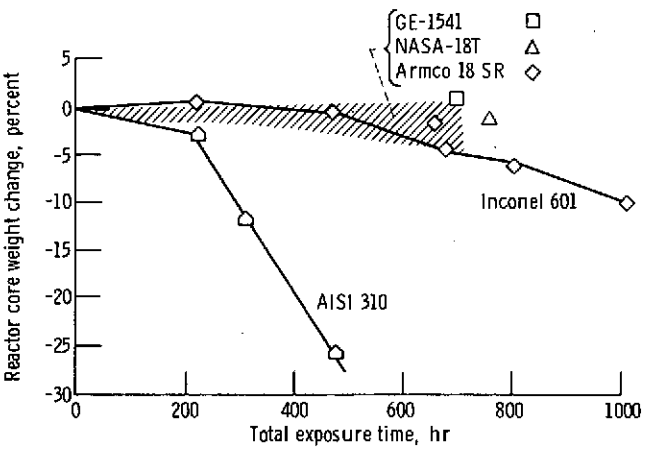

Figure 14. - Performance of uncoated alloys in an automobile thermal reactor endurance test.

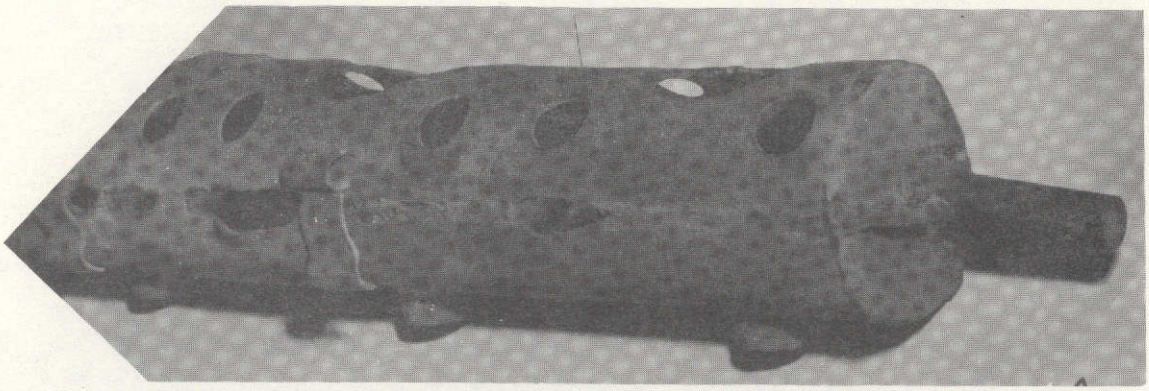

(a) Exposure, 440 hours. X1.

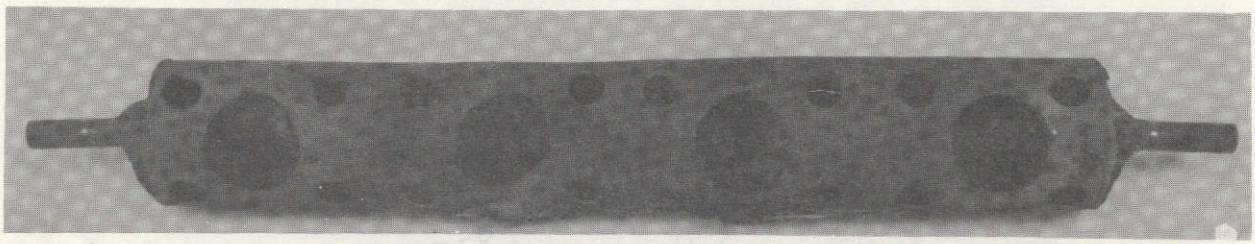

(b) Exposure, 650 hours. X1/3.

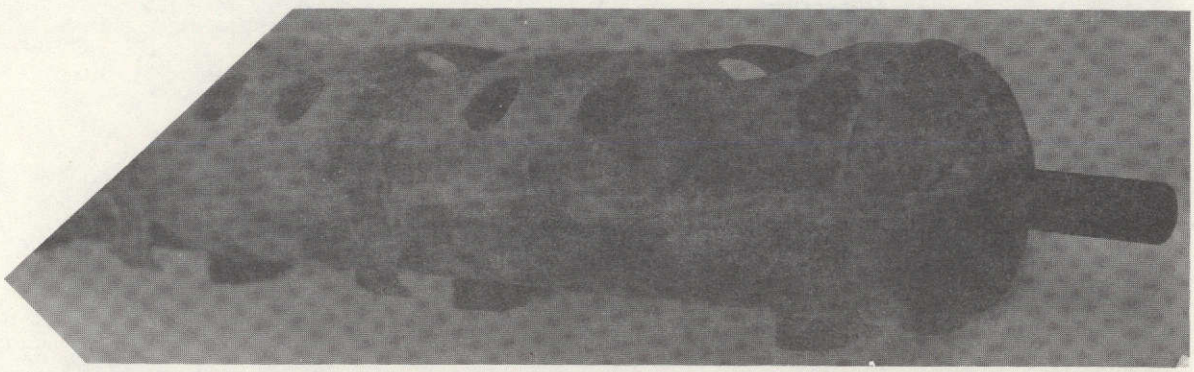

(c) Exposure, 684 hours; W-1 weldments. X1.

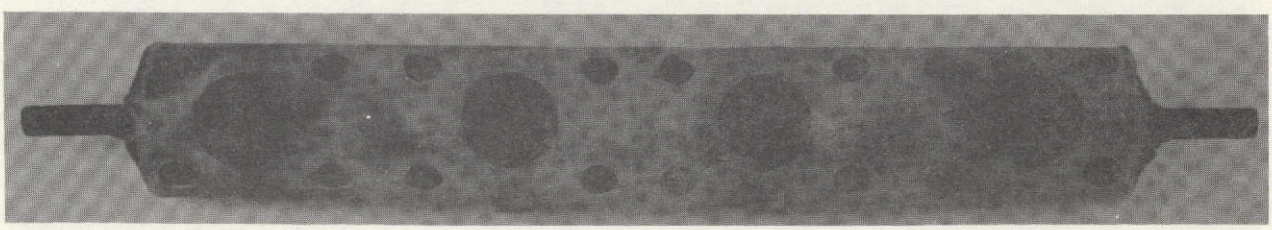

(d) Exposure, 684 hours; W-1 weldments. X1/3.

Figure 15. - GE-1541 reactor cores after exposure to endurance test.

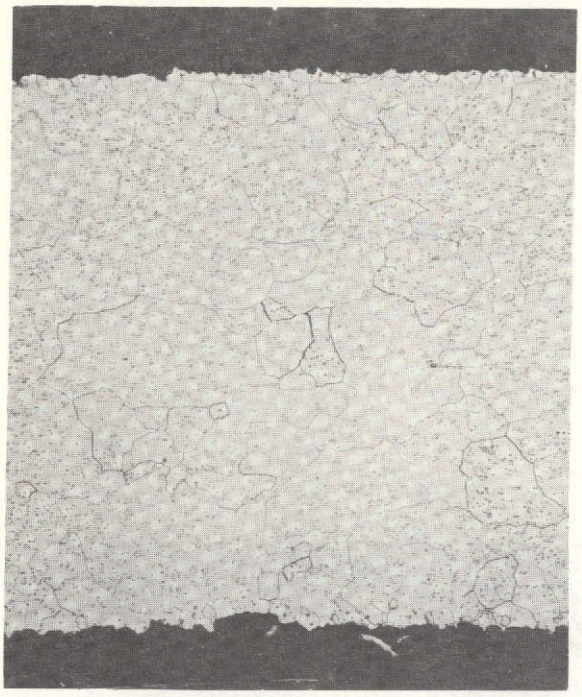

(a) GE-1541. X50.

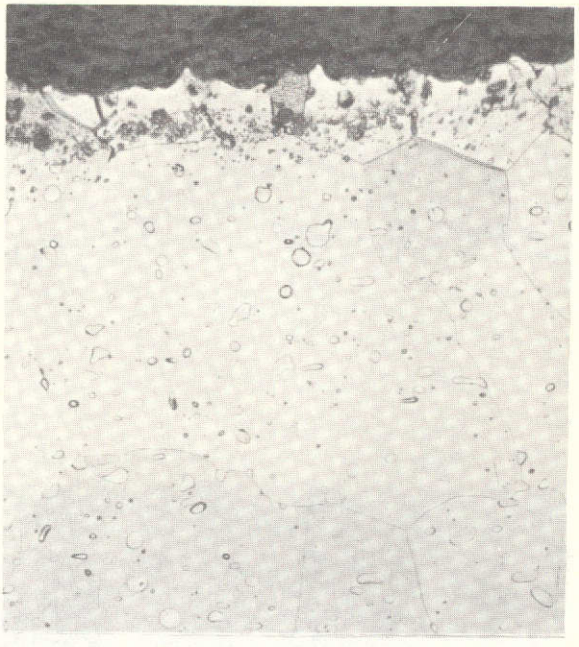

(b) GE-1541. X250.

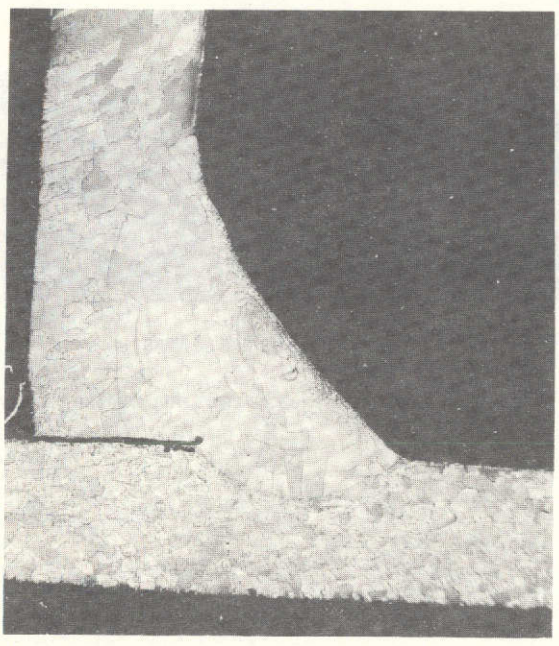

(c) GE-1541; W-1 weld at thermocouple stud. X10.

Figure 16. - Photomicrographs of GE-1541 reactor core after exposure to 684-hour endurance test.

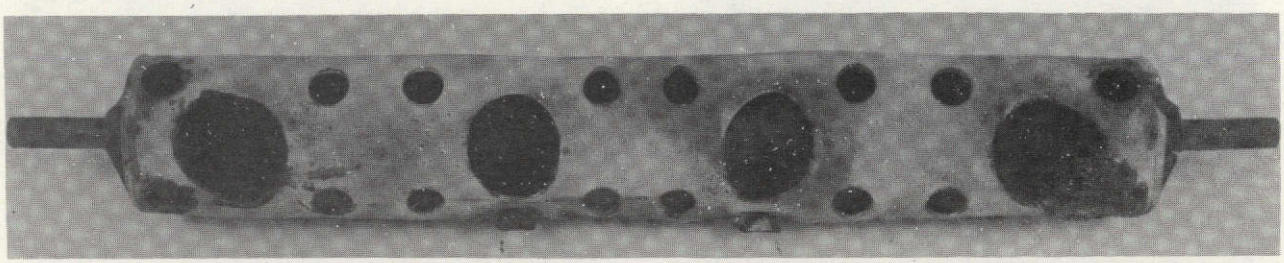

(a) Armco 18 SR after 616 hours.

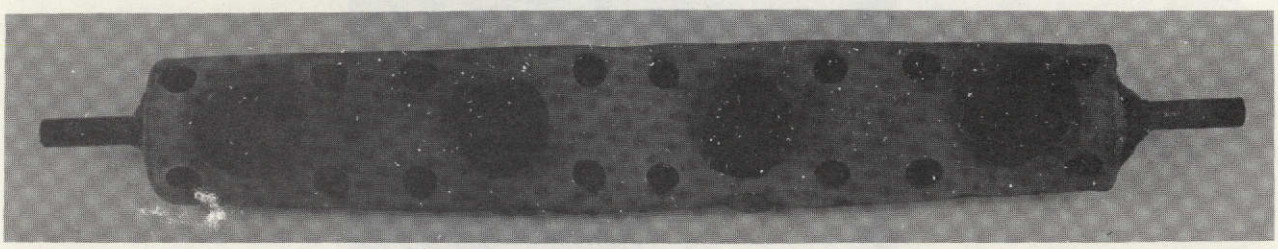

(b) NASA-18T after 762 hours.

Figure 17. - Armco 18 SR and NASA-18T reactor cores after exposure to endurance test. X1.

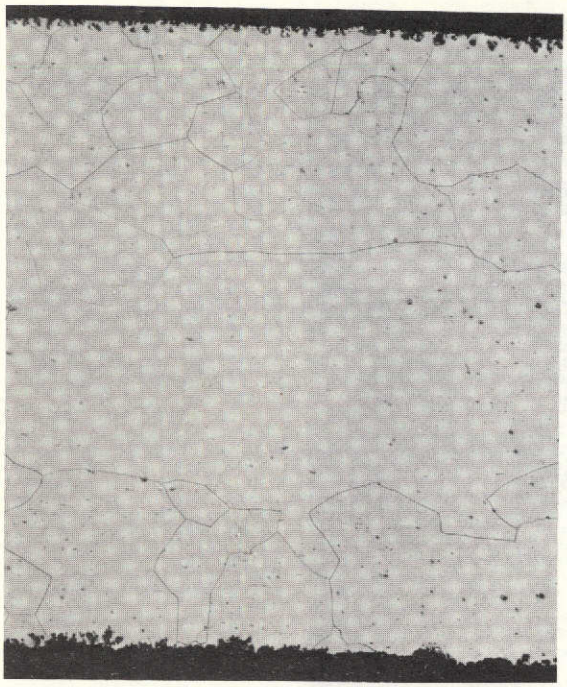

(a) Armco 18 SR after 616 hours. X50.

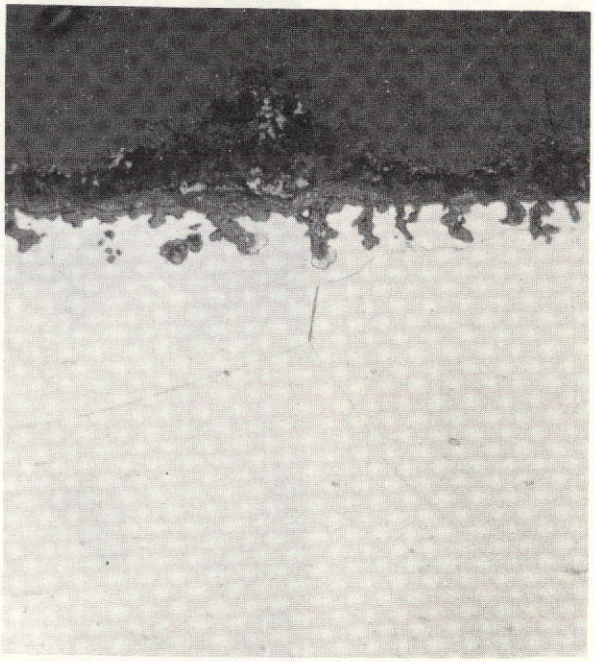

(b) Armco 18 SR after 616 hours. X250.

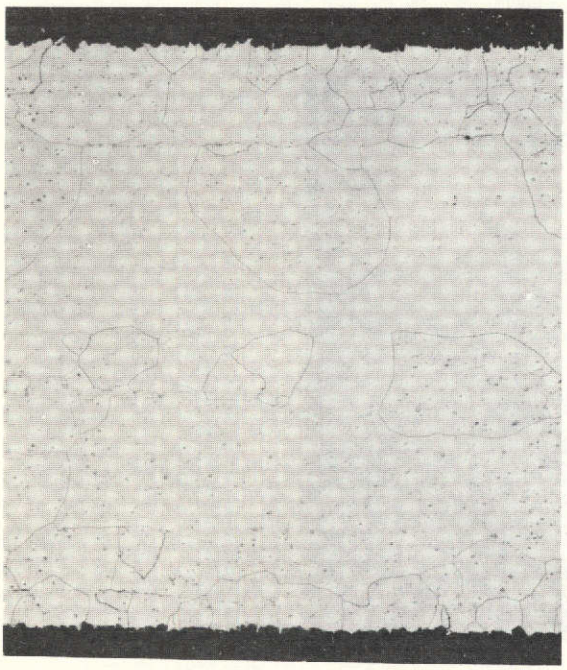

(c) NASA-18T after 762 hours. X50.

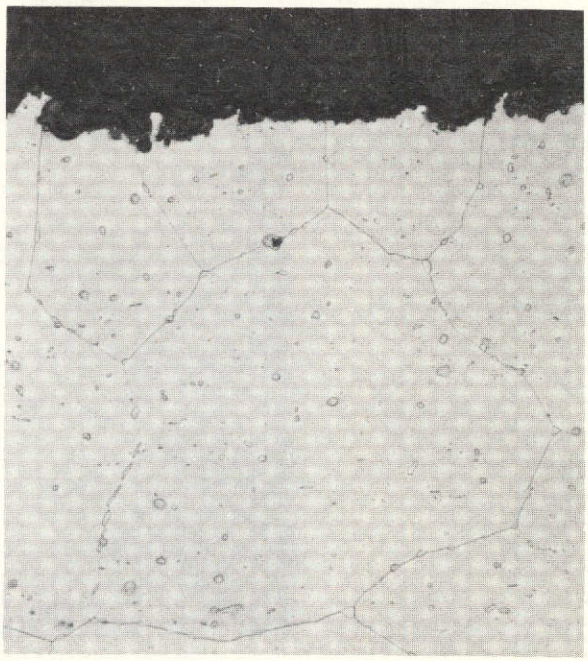

(d) NASA-18T after 762 hours. X250.

Figure 18. - Photomicrographs of Armco 18 SR and NASA-18T reactor cores after exposure to endurance test.

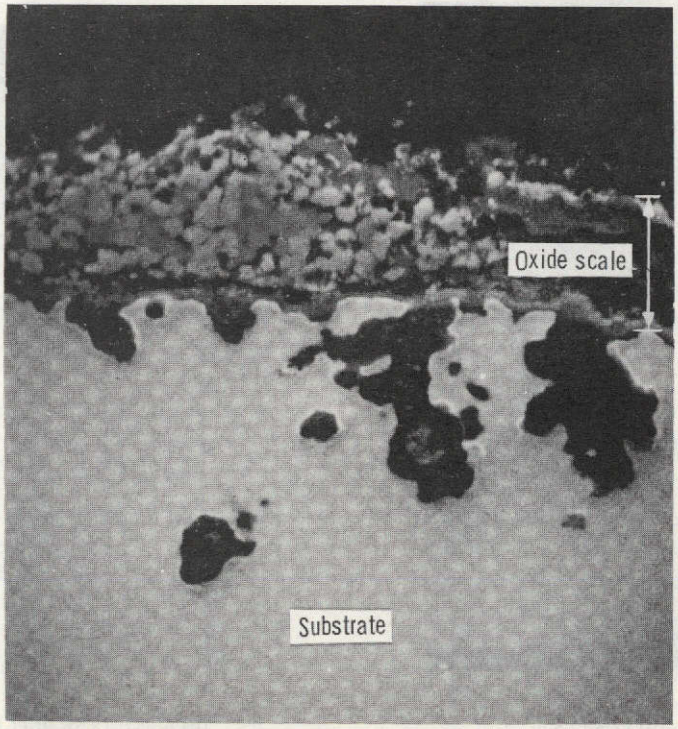

(a) Armco 18 SR after 616 hours.

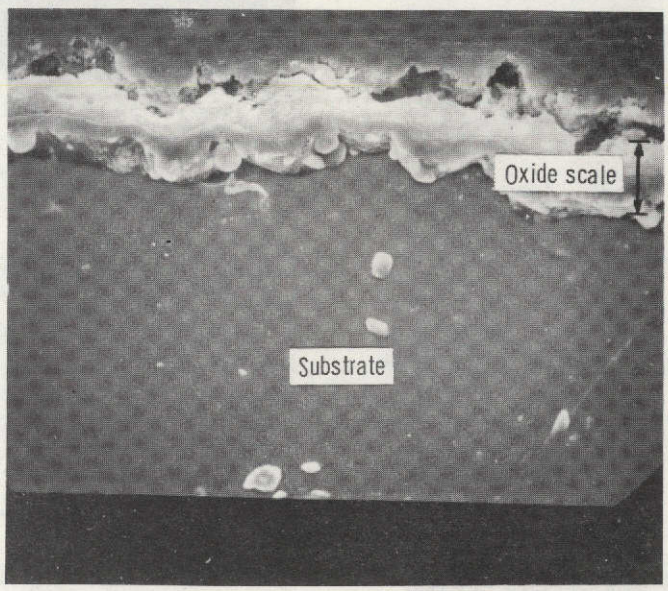

(b) NASA-18T after 762 hours.

Figure 19. - Scanning electron photomicrographs showing oxide scales formed on Armco 18 SR and NASA-18T after exposure to endurance test. X1000.

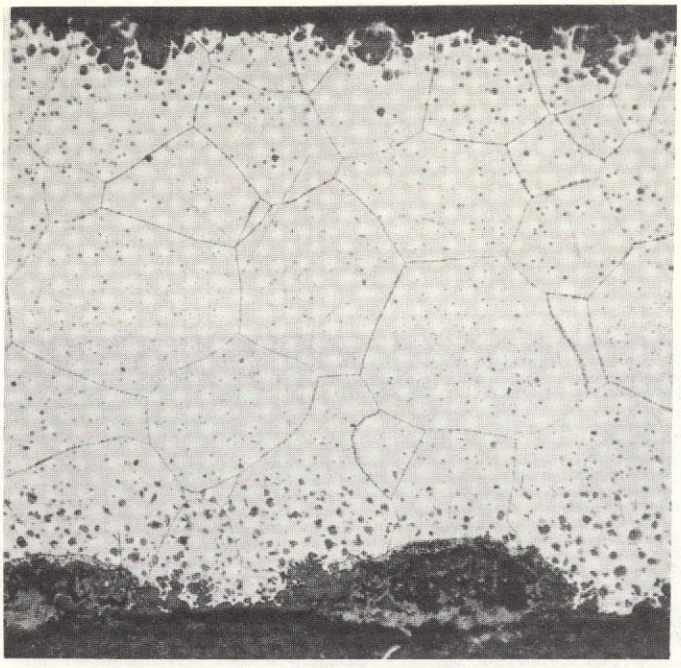

(a) NASA-15T after 404 hours.

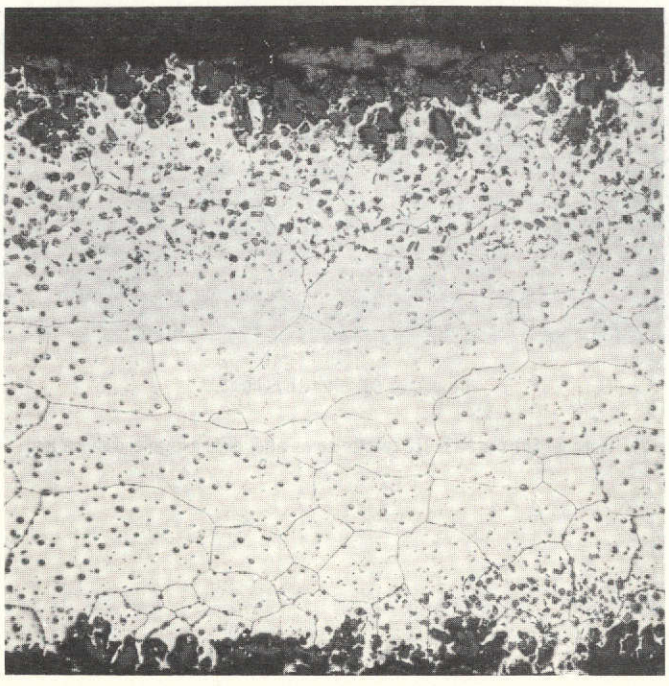

(b) NASA-15T2 after 470 hours.

Figure 20. - Photomicrographs of NASA-15T and NASA-15T2 reactor cores after exposure to endurance test. X50.

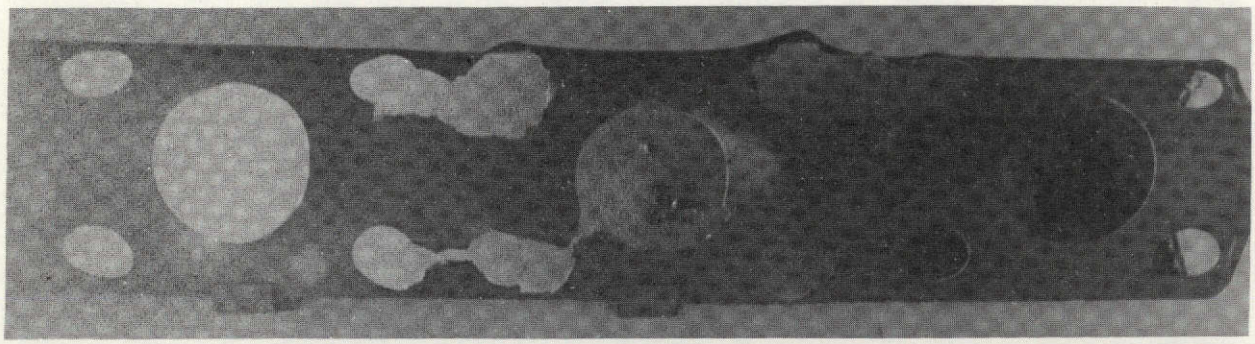

(a) AISI 310 after 585 hours.

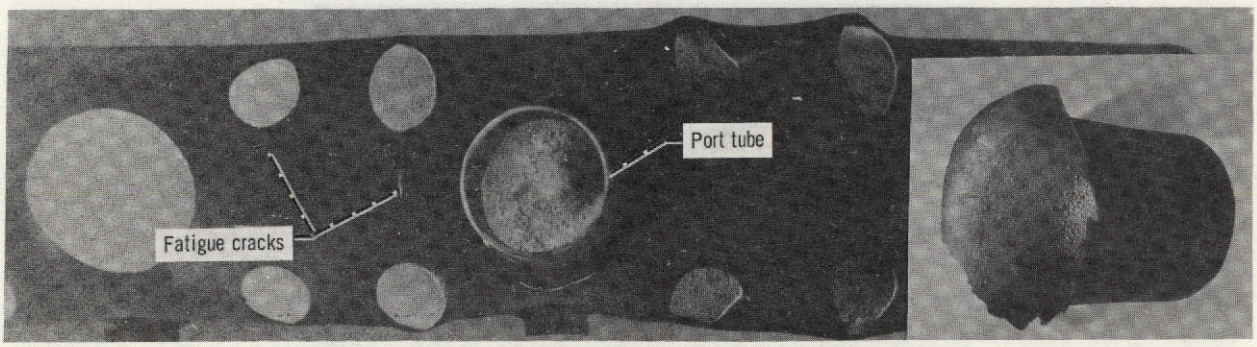

(b) Inconel 601 after 1000 hours.

Figure 21. - Inconel 601 and AISI 310 reactor cores after exposure to endurance test. X1.

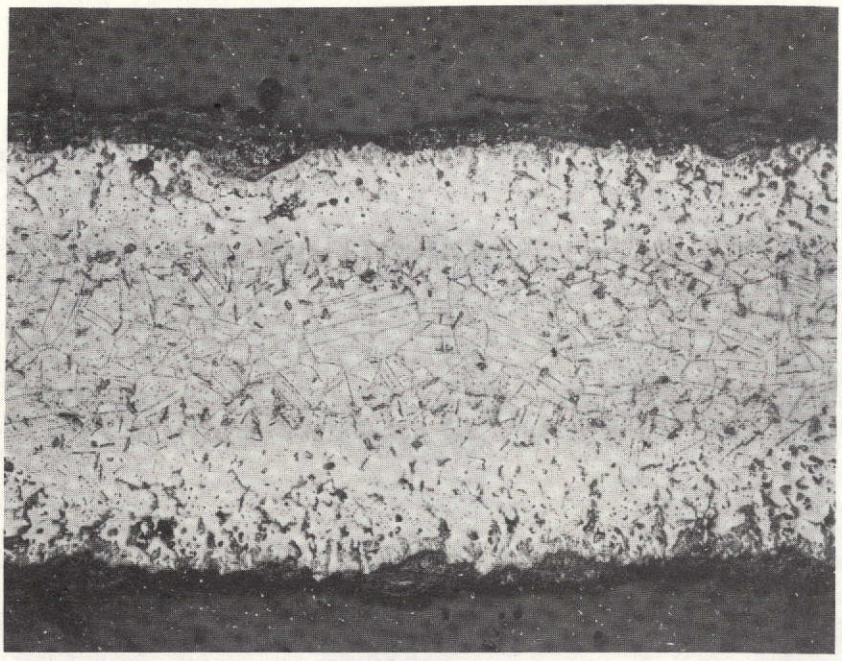

(a) Core section. X50.

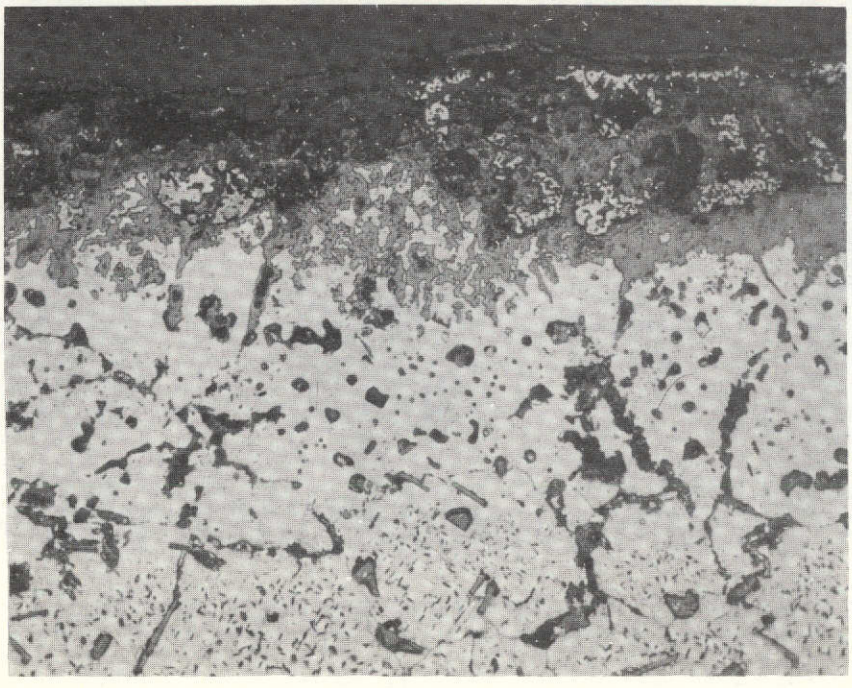

(b) Core surface. X250.

Figure 22. - Photomicrographs of Inconel 601 reactor core after exposure to 1000-hour endurance test.

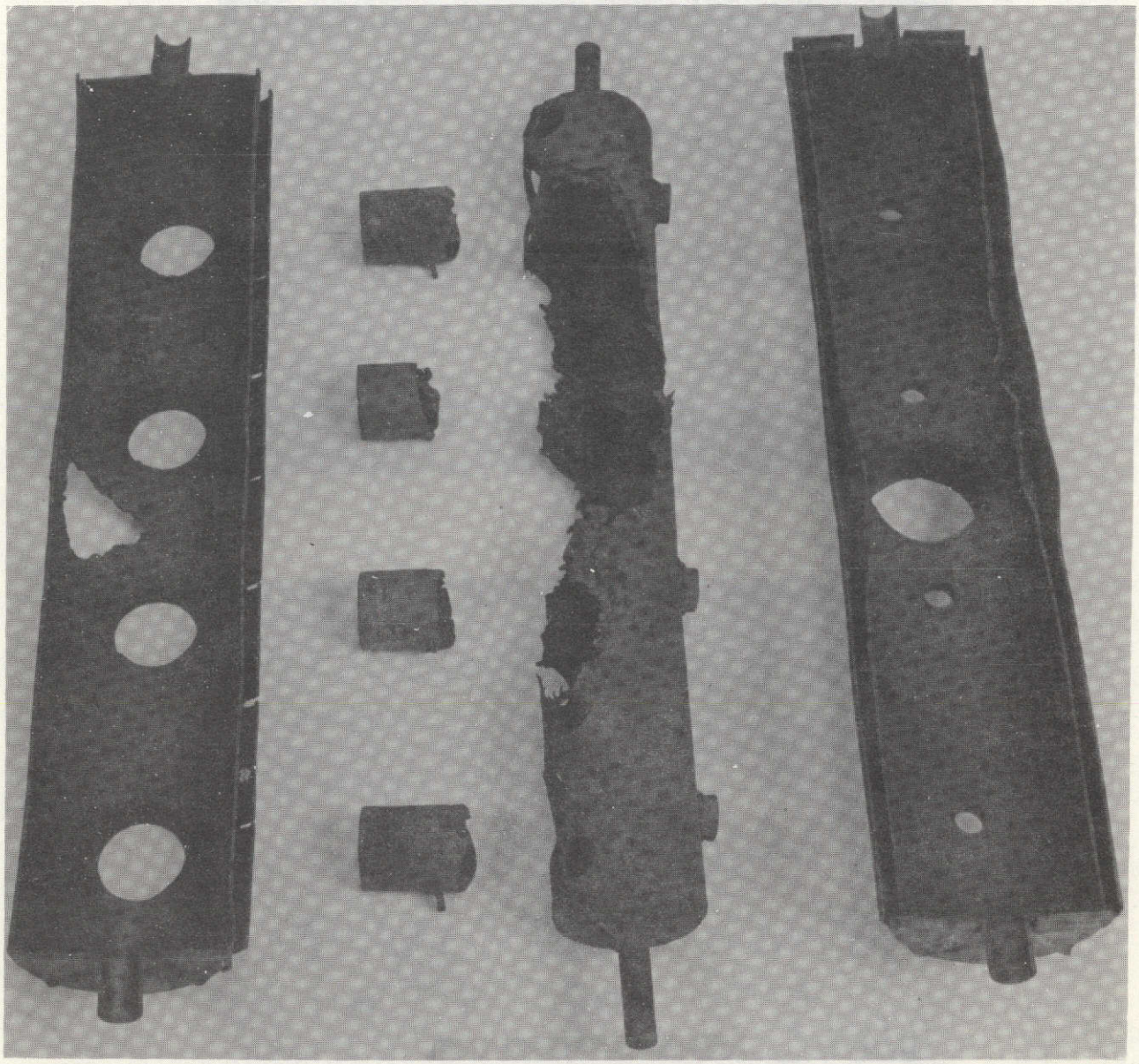

Figure 23. - NC-9/AISI 651 coated reactor components after exposure to 325-hour endurance test.

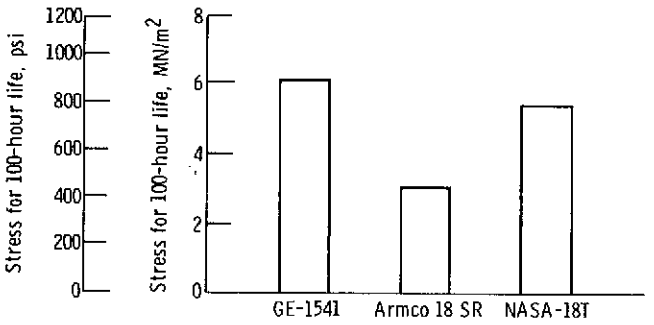

Figure 24. - Comparison of stress-rupture properties of three ferritic-iron alloys at 1000^0 C (1830^0 F).